National Library of Canada
Acquisitions and Bibliographic Services Branch
395 Wellington Street
Ottawa, Ontario
K1A 0N4

Bibliothèque nationale du Canada
Direction des acquisitions et des services bibliographiques
395, rue Wellington
Ottawa (Ontario)
K1A 0N4

Your file Votre référence

Our file Notre référence

NOTICE

The quality of this microform is heavily dependent upon the quality of the original thesis submitted for microfilming. Every effort has been made to ensure the highest quality of reproduction possible.

If pages are missing, contact the university which granted the degree.

Some pages may have indistinct print especially if the original pages were typed with a poor typewriter ribbon or if the university sent us an inferior photocopy.

AVIS

La qualité de cette microforme dépend grandement de la qualité de la thèse soumise au microfilmage. Nous avons tout fait pour assurer une qualité supérieure de reproduction.

S'il manque des pages, veuillez communiquer avec l'université qui a conféré le grade.

La qualité d'impression de certaines pages peut laisser à désirer, surtout si les pages originales ont été dactylographiées à l'aide d'un ruban usé ou si l'université nous a fait parvenir une photocopie de qualité inférieure.

Canada

IDENTIFICATION OF TIME-VARYING HUMAN JOINT DYNAMICS DURING AN ELECTRICALLY STIMULATED TWITCH

James P. Trainor

A Thesis submitted to
the Faculty of Graduate Studies and Research
in partial fulfillment of the requirements for the degree of
Master of Engineering

Biomedical Engineering Department
&
Department of Mechanical Engineering
McGill University, Montreal

June 1994

ISBN 0-612-05481-0

Abstract

The neuromuscular system interacts with the environment by generating forces that cause motion about joints. The study of this interaction is termed *joint dynamics*. If the environment is controlled, as it is in experimental situations, then it is possible to draw conclusions concerning the nature of the intact neuromuscular system by studying the nature of environmental interactions; i.e., by studying joint dynamics. The properties of the neuromuscular system, as manifested by the dynamic properties of joints, vary through time as a result of variations in the state of the physiological structures involved. Identifying the time-varying dynamics of joints under controlled circumstances is an important step in the development of a comprehensive model of the neuromuscular system.

This thesis presents the results of applying a method of nonparametric time-varying linear system identification to study the dynamics of the ankle joint as they vary during a single twitch of the triceps surae muscle group. In accord with previous time-invariant, and time-varying studies, the nonparametric results were characterized using a second-order model. Past studies have found that second-order models successfully characterize joint dynamics under time-invariant conditions. Time-varying studies have, however, found that second order models do not adequately characterize time-varying joint dynamics. The results presented here confirm that. Furthermore, examination of the reasons for this failure leads, with tentative analytic corroboration, to the conclusion that a fourth order linear model is required to characterize the time-varying dynamics of joints.

Résumé

Le système neuro-musculaire interagit avec l'environnement extérieur en générant des forces causant des mouvements autour des joints. On appelle *dynamique des joints* l'étude de ce type d'interaction. En contrôlant l'environnement, sous conditions expérimentales, il est possible de tirer des conclusions concernant la nature intrinsèque du système neuro-musculaire par l'observation des interactions environnementales; i.e., par l'étude de la dynamique des joints. Les propriétés du système neuro-musculaire, qui se manifestent par l'entremise des propriétés dynamiques des joints, varient temporellement dû aux variations d'état des structures physiologiques impliquées. L'identification de la dynamique des joints soumise à des variations temporelles, sous des conditions controllées, est un prérequis important pouvant éventuellement mener à l'élaboration d'un modèle complet du système neuro-musculaire.

Cette thèse présente les résultats obtenus suite à l'utilisation d'une méthodologie d'identification non-paramétrique de systèmes linéaires des joints de la cheville. Et ce, durant leurs variations faisant suite à un simple tic nerveux du groupe tricep surae. En accord avec des études précédentes, à la fois en conditions statiques et à variations temporelles, les résultats sont caractérisés par un modèle de second ordre. Les études sous conditions statiques ont démontré que les modèles de second ordre offrent une bonne caractérisation de la dynamique des joints sous de telles conditions. Par contre, les études sous conditions de variations temporelles démontre que les modèles de second ordre ne caractérisent pas de façon adéquate la dynamique des joints soumise à des variations temporelles. Les résultats présentés dans cette thèse confirment cette conclusion. L'impossibilité d'utiliser le modèle de second ordre afin de caractériser les résultats non-paramétriques, démontre qu'un modèle de quatrième ordre est requis pour caractériser la dynamique des joints sous conditions de variations temporelles. Une ébauche analytique qui tend à appuyer cette conclusion est offerte dans le présent document.

Table of Contents

Abstract i

Résumé ii

Table of Contents iii

List of Figures v

1 Introduction 1

2 Background 5

2.1 Muscle Morphology 5

2.2 Muscle Mechanics 6

2.3 Motor Control 11

2.4 Joint Dynamics 15

2.5 Functional Neuromuscular Stimulation 21

3 Theory 25

3.1 Time-Varying System Identification 25

3.1.1 Survey of Theoretical Techniques 26

3.1.2 Applications 34

3.2 Interpreting the Time-Varying Convolution Integral 36

3.3 Solution of the Time-Varying Convolution Integral 40

3.3.1 Correlation Based Solution 40

3.3.2 Pseudo-inverse Solution 42

4 Experimental Procedures and Analysis 45

4.1 Paradigm 45

4.2 Apparatus 45

4.3 Analysis 48

4.3.1 Pre-processing 48

4.3.2 Post-processing 52

4.3.3 Overall Analysis Procedure 58

5 Results 59

6 Discussion 83

7 Conclusions 91

Appendix A 93

References 94

List of Figures

2.1 Plot of single twitch, unfused tetanus, and tetanus. 8

2.2. Length-Tension relationship. 9

2.3 Force-Velocity relationship. 11

2.4 Block structure model of reflex mechanisms. 15

2.6 (a) Ankle stiffness gain. 19

2.6 (b) Variation of stiffness with mean torque. 19

2.7 FNS stiffness control scheme. 22

3.2 Weighting function versus impulse response function. 37

4.1 Artifact suppression circuit. 47

4.2 Normalized low frequency stiffness. 55

4.3 Overview of analysis. 58

5.1 Ankle torque during twitch. 59

5.2 Torque, position, and EMG during typical twitch. 61

5.3 Position/Torque power spectrum. 62

5.4 Ensemble of 10 torque recordings during twitch. 63

5.5 Ensemble of 10 position recordings during twitch. 64

5.6 Ensemble torque and position mean. 66

5.7 Ensemble torque and position with mean removed. 67

5.8 Time-varying stiffness impulse response function, data set one. 69

5.9 Time-varying stiffness impulse response function, data set two. 70

5.10 Time-varying stiffness impulse response function, data set three. 71

5.11 Time-varying stiffness impulse response function, data set four. 72

5.12 VAF of time-varying stiffness impulse response function. 73

5.15 Change in std. of torque, versus drop in VAF during twitch. 74

5.14 Time-varying low frequency average stiffness. 75

5.15 Time-varying compliance impulse response function for data set one. 77

5.16 Time-varying compliance impulse response function for data set two. 78

5.17 Time-varying compliance impulse response function for data set three. 79

5.18 Time-varying compliance impulse response function for data set four. 80

5.19 Time-varying second-order parameters. 82

6.1 Compliance IRF at 250ms after twitch. 86

6.2 Compliance IRF at 250ms after twitch with finite order IRF's. 86

6.3 System order estimate through time, data set one. 88

6.4 System order estimate through time, data set two. 88

6.5 System order estimate through time, data set three. 89

6.6 System order estimate through time, data set four 89

1 Introduction

The basis of all human motion is the interaction of two elements: the neuromuscular system, and the environment.

The dynamic properties of many systems in what we call the *environment* are, for practical purposes, well understood, and the laws of physical science are largely successful when applied *a priori* to model the dynamic properties of many of the systems one may wish to understand. The desire to understand these systems stems from the practical benefits gained when one learns to manipulate them; and it is much easier to manipulate a system that is understood than it is to manipulate one that is not.

When we can't, or won't, manipulate the environment ourselves, humans build things to do it for them: structures, mechanisms, circuits, *devices*. All these *devices* succeed because we understand how they interact with the environment.

Understanding how the neuromuscular system behaves in the real world benefits from a similar approach — that is, developing an understanding of the nature of environmental interactions. These interactions are described by a property of the neuromuscular system referred to as joint dynamics. Complete understanding of the nature of the neuromuscular system as manifested by the dynamic characteristics of a joint requires more than a morphological description of the system. It requires a model, like that used to describe a *device*, which predicts outputs given inputs. In the case of a joint, the inputs and outputs can be any combination of external (i.e., environmental) forces applied to the joint, passive internal forces resulting from the mechanical characteristics of tissue, active internal forces generated by the contractile muscle tissue in response to neural activation, and motion about the joint. A model of the dynamics of a joint describes the relationship between force and motion about the joint and elucidates the function of, and relationship between, all the components of the neuromuscular system.

Developing such a model presents some difficulty because, unlike most of the devices used to construct physical systems, there does not exist a sufficient first principles framework from which a comprehensive model of the neuromuscular system can be constructed.

Some characteristics of the neuromuscular system have been modeled successfully using empirical measures. For example Hill's force-velocity relationship (Hill, 1938) is

an empirical model that accurately describes a single property of muscle — the relationship between force and shortening velocity.

Methods of system identification have been applied successfully to study the intact neuromuscular system. Models of joint dynamics identified in this way are, like Hill's relationship, essentially empirical models that describe the behavior of the system under a restricted circumstance — that under which the data used to identify the system was collected.

In particular, nonparametric methods of system identification prove useful because they require no *a priori* assumptions concerning the nature of the system other than those demanded by the mathematical framework of the identification technique. This property of nonparametric models is considered valuable when studying a system as complicated as the neuromuscular system for which a complete first principles framework, from which to develop a parametric model, does not exist (Kearney and Hunter, 1990).

Nonparametric system identification techniques are broadly classified by two characteristics: linearity, and time variance. Therefore, four types of models can be identified: linear time-invariant, linear time-varying, nonlinear time-invariant, and nonlinear time-varying.

Linear time-invariant models successfully model joint dynamics under time-invariant conditions. Such models hold only when the state of the neuromuscular system is the same as that under which the model was identified. In this context, the state of the system is the position of the joint, and the mean level of voluntary muscle activation. Linear time-varying models have been applied to study joint dynamics as the state of the neuromuscular system varies through time. In these scenarios the position of the joint, or the level of voluntary activation, is intentionally varied.

Time-invariant conditions are the simplest to study, and the results are the simplest to interpret. Time-invariant results provide a basis from which to interpret time-varying results. Comparing the results of time-invariant and time-varying studies leads to a better understanding of the requirements of any theory that strives to characterize the neuromuscular system accurately.

Nonparametric models are purely empirical descriptions of the neuromuscular system. They are founded more on principles of mathematics, than on laws of physics. Because of this, the results can be difficult to *interpret*, and if the results are difficult to interpret

then it becomes difficult to draw significant conclusions. For this reason it is necessary to find an appropriate means to *characterize* the nonparametric findings. To draw significant conclusions about a physical system it is helpful then to characterize the results using some form of physical model.

Time-invariant studies conclude that a second-order model (commonly used in almost every branch of physical science) is adequate to characterize the results of time-invariant studies (Kearney and Hunter, 1990). Time-varying studies have, naturally, attempted to characterize their results with the same type of model, but evidence suggests that when the state of the system varies a second-order model is no longer adequate to characterize the results (e.g., MacNeil et al., 1992).

The time-varying studies conducted to date have studied the neuromuscular system during imposed motion, and time-varying voluntary activation. Both of these paradigms generate a response that incorporates the properties of passive tissues (i.e., muscle and connective tissue), active muscle tissue, voluntary activation, and involuntary activation (i.e., reflexive neural input).

It is desirable to narrow the response of the intact neuromuscular system to just that of the passive tissues, and active muscle tissue (i.e., no voluntary or reflexive neural input). This is possible by activating the muscle artificially, and is the course taken in the experiments presented in this thesis. The response studied in this thesis is a single electrically stimulated twitch of the triceps surae muscles. The state of the neuromuscular system during the twitch is examined by identifying the time-varying dynamics of the ankle joint during the twitch.

The motivation for performing such an experiment is not to answer a single overwhelming question, or to settle a particular dilemma definitively. The motivation is to build on a legacy of basic research that has considered basic questions to develop a body of knowledge of sufficient scope to propose models of the neuromuscular system which hold beyond the constraints of a particular experimental situation.

The thesis is presented in six sections:

The *Background* section reviews the important aspects of muscle morphology and mechanics, followed by a discussion of the neuromuscular mechanisms underlying motor control and the stiffness regulation hypothesis. This leads to a discussion of joint dynamics and a short discussion of one application that draws from these areas of study, that of functional neuromuscular stimulation.

The *Theory* section presents the analytical basis, and applications of, four techniques available for the study of time-varying systems. These are: quasi-time-invariant methods, adaptive methods, ensemble methods, and finally functional expansion methods. The remainder of this section focuses on discussion of the time-varying convolution integral, and the ensemble method of solution.

The *Experimental Procedures and Analysis* section explains the experimental paradigm — identification of the dynamics of the ankle joint during a single electrically stimulated twitch of the triceps surae muscles — and includes a detailed discussion of the analysis. The analysis section is presented in two parts: the pre-processing steps required before application of the ensemble identification method, and post-processing performed to interpret those results.

The *Results* section presents and discusses the results of the analysis of four experimental data sets. This section presents examples of the raw data, and how it was transformed (i.e., pre-processed) before application of the ensemble identification method. A complete set of results is presented for each set of experimental data.

The *Discussion* section considers the findings presented in the results section and how they reflect on previous related research. The discussion revolves around the use of parametric models as a method of characterizing joint dynamics, and in particular, the apparent failure of second order models under time-varying conditions. The discussion concludes with evidence pointing to the need for a third or fourth order parametric model to characterize time-varying joint dynamics.

Finally, the *Conclusion* section summarizes the results, and makes a concise statement of future research directions pointed to by the findings presented in this thesis.

2 Background

There are three types of human muscle: smooth, cardiac, and skeletal. Smooth muscle is a major component of the muscular internal organs, cardiac tissue is the muscle of the heart, and finally, skeletal muscle is that which is connected to the skeleton by tendons and causes motion about joints. Although all muscle types share the same basic elements, such as the contractile proteins which are responsible for force generation, they are all morphologically different. The following material reviews the basic properties of just one of these, skeletal muscle, and the neuromuscular systems which control it.

2.1 Muscle Morphology

Muscle exists as a hierarchy of physiological structures, whole muscle, existing on a scale of up to several tens of centimeters in length, to the basic contractile proteins which exists on a scale of just a few μm.

Whole Skeletal Muscle

At the highest level of organization, muscle is composed of an outer sheath of connective tissue, composed of collagen, that is continuous with the muscle's tendons and connects the muscle to the skeleton. Attachment occurs across joints so that contraction of skeletal muscle always produces torque about one or more joints. Connective tissue serves to join and contain bundles of individual muscle fibers, and further, to join and contain the collection of muscle fibers which make up the muscle.

Muscle Fibers

Muscle fibers are individual cells that can span the entire length of the muscle and have diameters ranging from 10 to 100 μm. A muscle may contain from a few hundred to several thousand fibers (Schauf, 1990). Muscle fibers are the level at which the nervous system innervates skeletal muscle and are generally classified in three groups: (i) slow oxidative fibers, (ii) fast oxidative fibers, and (iii) fast glycolytic (Schauf, 1990). The classifications are based on the fiber's contractile (fast/slow), and metabolic (oxidative/glycolytic) properties, and, the distinctive properties of each fiber are pertinent in explaining the manner in which the central nervous controls muscle activation depending on task exigencies (see section 2.3).

Myofibrils and Sarcomeres

Muscle fibers are made up of long parallel myofibrils which are 1-2 μm in diameter. When viewed under a microscope myofibrils present a banded structure of repeating sub-units called sarcomeres. Individual sarcomeres are recognized as the basic force generating elements of muscle. A relaxed sarcomere is 1.5 to 2.0 μm, but as a muscle contracts the sarcomeres actively shorten, and as a muscle extends the sarcomeres actively lengthen. This theory of force generation is known as the sliding filament theory. The overall force generating properties of a muscle are the result of interaction of the active properties of sarcomere, with the passive properties of the muscle's connective tissue structures (Schauf, 1990; McMahon, 1984, Huxley, 1974).

Myofilaments and Contractile Proteins

Sarcomeres are composed of inter-digitating thin and thick filaments, collectively known as myofilaments, which interact to develop force and effect shortening of the muscle. The sliding filament theory describes the mechanism by which the thick and thin filaments slide across one another to effect shortening of individual sarcomeres. It postulates that the thick and thin filaments slide across one another by the action of physical links that generate force during contraction. The force generating links between thick and thin filaments are termed cross bridges, and come about by molecular interactions between the protein molecules of which the thin and thick filaments are made.

Thick filaments are about 1.5 μm long, 15 nm in diameter, and are composed of several hundred myosin molecules. Thin filaments are comprised of helical strands of globular actin molecules with sites approximately every 2.7 nm where myosin molecules can bind. Under a complex series of biochemical reactions, initiated by an inrush of calcium ions when a muscle fiber membrane depolarizes, the actin and myosin molecules go through a cyclical reaction which first binds the molecules, next passes them through a state transformation which causes relative motion between the thin and thick filaments, and finally breaks the bond so that the process can repeat itself.

2.2 Muscle Mechanics

The study of muscle in vitro is the first step in understanding how the neuromuscular system controls muscles to accomplish tasks. The fundamental reactions which describe

a muscle behavior are: (i) *stretch* in response to external loads, and (ii) *contraction* in response to stimulation by the central nervous system (or in response to some artificial external stimulus). These two responses are described in terms of two basic properties: passive mechanical properties, and active mechanical properties.

Passive Mechanics

The most basic mechanical property of muscle that can be measured is its resistance to an imposed stretch. In isolated muscle that is not undergoing any form of stimulation (and therefore generating no active force) this resistance can only be due to the passive structures of the muscle. As is the case with engineering materials, resistance to imposed changes in length is termed stiffness. If an isolated muscle is stretched to a number of constant lengths, and the force recorded, one finds that the curve relating displacement to force grows steeper with increasing displacement. The stiffness of the passive tissues, therefore, increases with displacement; the passive tissues exhibit nonlinear elastic properties. This behavior is characterized (in terms of force, F, and displacement, x) by the differential equation (Winters, 1990):

$$\frac{dF}{dx} = K_1F + K_2 \qquad 2.1$$

which has the solution:

$$F = K_3(e^{K_1x} - 1) \qquad 2.2$$

Where K_i are constants. This empirical equation characterizes the elastic properties for many collagenous tissues including skin, tendon, passive cardiac muscle, and passive skeletal muscle. However, as is the case with many areas of muscle mechanics, no plausible derivation from first principles has yet been discovered (McMahon, 1984). This relationship is shown in figure 2.2 and is termed the passive length-tension property.

Active Mechanics

When the membrane of a muscle fiber is depolarized, that fiber's contractile machinery activates to effect a single transient mechanical event. If isolated whole muscle is stimulated electrically, a number of muscle fibers (in proportion to the strength of the stimulus) will activate in synchrony to produce a twitch, such as that shown in figure 2.1.

relationship between force and rate of contraction is more complex than this — it is a matter of common experience, for example, that muscles shorten more rapidly against light loads than they do against heavy loads. Essentially, a muscle can produce less force when it is actively shortening than it can when it contracts isometrically (McMahon, 1984). A. V. Hill (1938) identified an inverse relationship between force and shortening velocity, and proposed equation 2.3, now known as Hill's equation (McMahon, 1984; Winters, 1990), as an empirical description of this behavior.

$$(F + a)(v + b) = (F_0 + a)\,b \qquad 2.3$$

Where F = muscle tensile force, F_0 = tetanic isometric force, v = muscle shortening velocity and, a and b are constants. The maximum shortening velocity, achieved under zero load, is then defined by: $v_{max} = \frac{b F_0}{a}$. Equation 2.3 can then be expressed in dimensionless form as:

$$\frac{v}{v_{max}} = \frac{1 - \frac{F}{F_0}}{1 + \frac{1}{k}\frac{F}{F_0}} \qquad 2.4$$

where $k = \frac{a}{F_0} = \frac{b}{v_{max}}$. This relationship has been found to describe cardiac, smooth, and skeletal muscle (McMahon, 1984). For most muscle k lies within the range $0.15 < k < 0.25$ (McMahon 1984). The force-velocity relationship for $k = 0.25$ is shown in figure 2.3.

During muscle lengthening the force-velocity relationship expressed by equation 2.3 does not hold. When muscle shortening speed is zero the muscle generates its maximum force it is capable of for a given activation level. This is referred to as isometric contraction. When the applied force is greater than the isometric force, the muscle will lengthen (i.e. negative shortening velocity) at a constant speed. The speed of lengthening under these conditions is much less than that predicted by Hill's force-velocity relationship. In fact, the slope of the force-velocity curve when muscle is lengthening is approximately six times greater than for muscle shortening (McMahon, 1984).

motoneuron can innervate hundreds, and even thousands, of muscle fibers. For example in the human medial gastrocnemius muscle the innervation ratio is approximately 1700 muscle fibers to one motoneuron (McMahon, 1984). Muscles performing delicate tasks, such as those controlling the fingers, have motor units consisting of as few as 2 or 3 muscle fibers (Schauf, 1990). While a single motoneuron innervates many muscle fibers, the opposite is not true, a muscle fiber is innervated by only one motoneuron. Motoneurons lie in the gray matter of the spinal cord and act as major point of integration for all motor signals directed at the motor unit. Each spinal motoneuron may receive as many as 15000 synaptic inputs (Schauf, 1990). Most of these inputs come from spinal inter-neurons, but a small fraction come directly from higher motor centers. The motoneurons are referred to as α motoneurons, and a group of motoneurons controlling a single muscle group are generally referred as an α-motoneuron pool.

Activation

Depolarization of a motoneuron causes an action potential to travel down the motoneuron axon finally reaching a muscle fiber, depolarizing the muscle fiber's membrane, causing the fiber to respond with a single twitch. Whole muscle is made up of an enormous number of muscle fibers controlled by a proportionally large number of motoneurons. If individual motor fibers respond with a twitch, why then is motion so fluid? The reason is that, under normal conditions, the motor units are desynchronized so that individual muscle fiber twitches sum to give smooth force development and fluid motion.

The summation of muscle fiber twitches, which ultimately modulates the force developed by a whole muscle, takes two forms: temporal summation, and recruitment. Temporal summation refers to the frequency of action potentials in the axons serving each active motor unit (Schauf, 1990). Force modulation of individual muscle fibers by temporal summation is conceptually the same as that in whole muscle tested in isolation and stimulated artificially — as shown in figure 2.1 — in which the force developed in the unfused tetanus state is a function of the rate of stimulation. Recruitment refers to size and number of motor units activated (Schauf, 1990) and formalizes the notion that not all of the motor units must be active over the full range of muscle force. Key to the recruitment axiom is the size principle. The largest motor units in a muscle are those which have the largest number of muscle fibers, and in turn the largest motoneurons. Similarly, the smallest motor units have the smallest number of muscle fibers and the smallest motoneurons. The level of stimulus required to depolarize a motoneuron is

proportional to the size of the neuron, therefore, as the motoneuron pool stimulus amplitude increases, small motor units are activated before large motor units. At low stimulus levels small motor units are recruited resulting in fine force resolution, as stimulus levels increase larger and larger motor units are recruited with a concomitant decrease in force resolution (McMahon, 1990). Together these mechanisms reconcile the environmental requirement of fine control over force and movement at low force levels with the requirement for powerful fast actions (requiring high force levels).

Muscle Proprioceptors

One set of significant inputs to the motoneuron pool are those from muscle proprioceptors. The two most significant muscle proprioceptors are the muscle spindles, and Golgi tendon organs. These organs sense, respectively, muscle length, and muscle force (Schauf 1990, McMahon 1984).

Muscle spindles are small receptors, sensitive to stretch, which are scattered throughout the body of a muscle. They consist of a capsule surrounding modified muscle fibers, called intrafusal fibers, to which several sensory afferent nerve endings are attached. Further, there are two types of intrafusal fibers: nuclear bag fibers, which have primarily group Ia afferent nerve endings, and nuclear chain fibers, which have group Ia and II afferent endings. The spindles operates in parallel with the muscle so that changes in muscle length cause corresponding changes in muscle spindle length. The spindles respond to these changes in length. A phasic length change (e.g. a quick stretch) provokes a response primarily from bag fibers, while a tonic change provokes a response primarily from chain fibers (Schauf, 1990). Thus, muscle spindles avail the CNS of both static and dynamic muscle length information.

Group Ia afferents from intrafusal fibers ascend to higher centers, and synapse with spinal inter-neurons and directly with α-motoneurons (Schauf, 1990). Intrafusal fibers are themselves innervated by γ-motoneurons, and will contract in response to γ-motoneuron activity. The γ input controls the sensitivity of muscle spindles over the entire range of muscle length. This is essential if contraction of the muscle is not to be accompanied by slackening of the spindles. A common notion is that when α-motoneurons are active (and the muscle is shortening), γ-motoneurons are coactive (Schauf, 1990; McMahon 1984). This compensatory input shortens the intrafusal fibers ensuring the muscle spindles remain loaded — the state they must be in to function properly as length sensors.

Golgi tendon organs exist in the tendons connecting muscle to the skeleton and function as force sensors. Golgi tendon organ afferents do not synapse directly with α-motoneurons, instead they synapse with spinal inter-neurons which then project to the motoneurons of the originating muscle, its synergists, and its antagonists. Activity in Golgi tendon organ afferents acts to inhibit the motoneurons of the originating muscle and its synergists, and excite the antagonist muscle motoneurons (Schauf, 1990). Early thought restricted the role of tendon organs to a reflex that inhibited muscle activity only when muscle force rose to unsafe levels. More recent evidence established that tendon organs respond to less than 0.1 g of force applied directly to the base of the organ capsule (McMahon, 1984).

Reflex and Regulatory Mechanisms

The efficacy of muscle spindles, and of the Ia synapses with α-motoneurons, is a matter of common experience for all those who have had their patellar tendon tapped by a physician. When the physician strikes the tendon the quadriceps muscle group is stretched a tiny amount. This tiny stretch is sufficient to cause the muscle spindles to fire, delivering a large input to the α-motoneuron pool, ultimately bringing it to threshold and causing the quadriceps muscle group to contract in response to the stretch.

Tendon organs are thought to be responsible for a less common but equally conspicuous reflex, which is most clearly seen in a decerebrate preparation, known as the clasp-knife-reflex. A decerebrate animal will exhibit an increase in muscle tone known as decerebrate rigidity. In this state, flexing the limb of the animal requires a great deal of force, but at a critically high level the limb will suddenly collapse. The reflex — in response to high force levels — is ostensibly the result of Ib afferent discharges by the Golgi tendon organs (McMahon 1984). This reflex is evidence of the role of Golgi tendon organs in protecting the system from unsafe force levels, but does not characterize their role in behavior at low force levels. At low force levels the tendon organs are thought to have a role in stiffness regulation (Nichols and Houk, 1975).

The Reflex Stiffness Hypothesis

Nichols and Houk (1975), present a schematic illustrating the origins of mechanical responses and reflex actions of the neuromuscular system. This is presented in figure 2.4, with adaptations by McMahon (1984) to include input from higher centers and γ-motoneurons. This schematic illustrates the mechanisms from which reflexes, such as

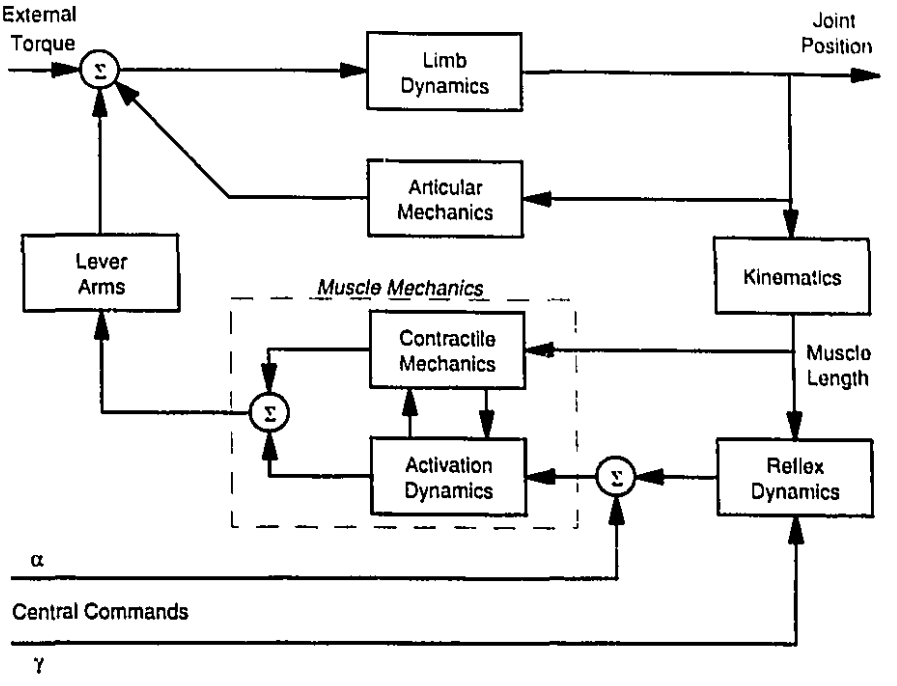

Figure 2.5. Block structured representation of information flow in the peripheral neuromuscular system (Kearney, 1990).

A Systems Approach

To understand how the disparate structures of the neuromuscular system come together to manifest joint dynamics, one must have a means of uniting the individual elements of the system. A logical approach is to build a block structured model of the system based on knowledge of how the underlying systems interact. Such a model is presented in figure 2.5, which models the underlying structures of the peripheral neuromuscular control system.

Some of the structures represented in figure 2.5 can be modeled accurately from *a priori* models, for example the limb dynamics can be modeled accurately, and with confidence, by application of Newton's laws. Other structures such as reflex dynamics or the two blocks labeled *Muscle Mechanics* cannot be accurately modeled *a priori* from a manageable set of first principles. These mechanisms can, however, be studied by applying the principles of system identification to characterize, (i) the overall input-output properties of the system, and (ii) the properties of individual elements in the system.

Position and torque are the only important signals that can be directly measured and manipulated in figure 2.5. (Neural input can be measured indirectly by measuring EMG.) Given measurements of joint position and torque, the relationship between the two — the joint dynamics — becomes a classic problem in system identification: obtain a model of the system through analysis of the relationship between input (position or torque), and output (torque or position) (Kearney and Hunter, 1990).

Stiffness Properties and Linear System Identification

Linear system identification methods have been used extensively to develop descriptions of joint dynamics of the ankle, wrist, elbow, jaw, and neck (Kearney and Hunter, 1990). The ankle joint, in particular, has been examined extensively using linear system identification by Gottlieb and Agarwal (1978), Kearney and Hunter (1982, 1990), Hunter and Kearney (1982), and Weiss et al. (1986a, 1986b, 1987). Gottlieb and Agarwal identified the compliance properties of the ankle joint, while the remainder identified, and considered in detail, the stiffness properties of the same joint. In general these experiments involve application of a small stochastic position perturbation about the ankle while the neuromuscular system is in a state defined by the experimental paradigm. Measurement of the torque generated in response to the position perturbation permits identification of the input-output properties by computing the frequency domain transfer function, or alternatively the time domain impulse response function, relating the two signals. Such a system model is termed a "stiffness" model because a position input is transformed to a torque output, alternatively a "compliance" model transforms a torque input to a position output.

Note, that figure 2.5 is structured as a compliance model, but an equivalent stiffness model could be had by simple rearrangement of the blocks and connections. Also note, that the stiffness referred to here is a full dynamic description of the relationship between position and torque, not the elastic, or static, stiffness as is commonly used to model a linear spring (i.e. force = elastic stiffness × displacement). Elastic stiffness is the zero order linear component of a system's dynamics (first and second-order terms would be, for example in a spring/mass/damper system, damping and inertia respectively). The distinction made here — between *elastic stiffness*, as the zero order term in the dynamics, and *stiffness*, as the full dynamic stiffness of the system — is maintained throughout this thesis.

Identification of a linear stiffness model requires determination of the transfer function:

$$\frac{Tq(s)}{\theta(s)} = H(s) \qquad 2.5$$

where Tq(s) is torque, θ(s) is angular position, and H(s) is the stiffness transfer function.

Alternatively, the time domain impulse response function:

$$Tq(t) = \int_{-\infty}^{\infty} h(\tau)\theta(t-\tau)d\tau \qquad 2.6$$

can be solved given input-output records θ(t), and Tq(t). The solution of equation 2.5 is discussed in detail by Bendat and Piersol (1986), the solution of equation 2.6 is discussed in detail by Hunter and Kearney (1983a).

Major Results

Kearney and Hunter (1990) have demonstrated that linear models provide an excellent description of joint dynamics provided that the state of the system (i.e. activation level, and mean position) remains constant over the period during which the dynamics are estimated. When the system is in a different state a linear model can still be identified but the identified model will not necessarily be the same. For example, dramatic changes in joint dynamics are apparent with variations in mean torque (i.e. activation level). This is illustrated in figure 2.6a which shows ankle stiffness transfer functions identified over a range of mean torques (activation levels). In this figure, increasing low frequency gain and increasing resonant frequency are clearly visible as mean torque increases.

The stiffness transfer functions presented in figure 2.6a can be numerically inverted to obtain compliance transfer functions. In this form individual gain curves bear resemblance to the classic second-order transfer function:

$$\frac{\Theta(s)}{Tq(s)} = \frac{G\,\omega_n^2}{s^2 + 2\zeta\omega_n s + \omega_n^2} \qquad 2.7$$

impulse response function (IRF, time domain representation of equation 2.7) to the nonparametric compliance IRF representing the dynamics of the ankle joint. Generally the parametric second-order compliance IRF represents the nonparametric compliance IRF very well (e.g., accounts for as much as 97% of the variance of the nonparametric IRF; Kearney and Hunter, 1990). Thus, equation 2.7 provides a parsimonious, easily interpreted, description of ankle joint dynamics under steady state conditions.

Weiss et al. (1986a, 1986b, 1988) investigated ankle stiffness over the full range of ankle position, and activation levels and presented the results in terms of the variation of second-order parameters with joint position and mean torque (i.e. activation level). Figure 2.6b is a representative result showing the variations of elastic stiffness with mean torque. The elastic stiffness varies considerably over the full range of activation, varying (in figure 2.6b) linearly from 40 Nm/rad at rest (0 Nm mean torque) to over 750 Nm/rad at maximum contraction (75 Nm mean torque). In contrast, the damping parameter, ζ, does not change significantly over the same range of activation, having a value of approximately 0.4 throughout. The natural frequency, ω_n, is related to elastic stiffness by the relation $\omega_n = \sqrt{K/I}$, where K = elastic stiffness, and I = inertia. The inertia of the joint does change with activation level or position, therefore, ω_n varies in proportion to the square root of elastic stiffness.

While it is intuitive that joint stiffness increases with contraction level, the linear relationship could not have been assumed *a priori*. A further significant property of the neuromuscular system which is not necessarily intuitive is that joint stiffness can, in fact, be controlled over a range of activation levels, such that the joint can present significant stiffness while at the same time presenting negligible torque. This behavior has potential functional significance which was recognized by Hogan (1984, 1985) who hypothesized that simple position or force control is not adequate to control dynamic interaction with the environment, and that one practical strategy is for the CNS to modulate the dynamic response (i.e. properties) of a joint, and by Lan et al. (1991a, 1991b), Crago et al. (1990, 1991) and Ning et al. (1991), who consider the application of stiffness regulation in functional neuromuscular stimulation as an effective strategy to control force and position in situations when transitions from position to force control, or vice versa, are required.

Open Questions

There are many situations in joint dynamics research when equation 2.6 is, however, not appropriate. The properties just discussed were the result of identification of joint

dynamics based on the application of small position perturbations to excite the system while it was in a steady state. Identification of equation 2.6 under these conditions is essentially linearization, at distinct operating points, of a system which is in general nonlinear and time-varying.

That the system is nonlinear is apparent if one identifies the linear dynamics using a series of position perturbations of varying amplitude. A linear system would yield the same estimates independent of perturbation size because the principle of superposition holds. Conversely, application of perturbations of varying amplitude to a nonlinear system will not yield identical linear estimates of the system dynamics. Such behavior has been observed in joint dynamics studies (Kearney and Hunter, 1982) and is a clear sign the underlying system in nonlinear. To identify such nonlinear properties a new class of system identification techniques must be brought to bear on the problem. Such techniques are not considered here. There are, however, quite active research efforts in the area (e.g. Hunter and Korenberg, 1986; Kearney and Hunter, 1988; Westwick and Kearney, 1990).

Equation 2.6 is also inappropriate for the identification of systems which vary through time. For example, if elastic stiffness varied quickly through time, equation 2.6 could not model the system even if it was completely linear. This is significant because even the simplest of natural motions involve continual changes in the state of the neuromuscular system, and hence time variations in joint dynamics. Appreciation of these variations is important in understanding fundamental properties of motor control, and in practical applications such as functional neuromuscular stimulation (FNS), which is discussed in the next section. Some results of the application of time-varying linear system identification techniques to problems in neuromuscular dynamics are discussed in section 3.1.2.

2.5 Functional Neuromuscular Stimulation

The significance of stiffness regulation by the neuromuscular system is apparent when one considers conclusions drawn in the study of FNS. The goal of FNS research is to restore motor function to individuals with neuromuscular injuries by direct activation of the paralyzed muscle. A FNS system is faced with the task of mimicking the neuromuscular system's behavior in a manner that produces natural motion, force regulation, and compliant interaction with the environment (Crago, 1983).

Lan (1990) added the feed forward element to the controller and referred to the controller as a *perturbation* controller. The feed forward element sets the controllers quiescent point, while the two feedback loops control against perturbations around that point.

Control systems theory provides a wealth of powerful techniques to optimize the design of a controller such as this, but all these tools require an adequate system model to predict the behavior of the overall system. The system elements of the controller which must be modeled are the muscle and limb dynamics. The limb dynamics are modeled using Newton's laws and, while perhaps not trivial, present no fundamental problems. For example, if the system is described in joint coordinates, i.e. $P_n = \theta_n$, then the limb dynamics can be written as:

$$T_n = I(\theta_n)\ddot{\theta}_n + c(\theta_n, \dot{\theta}_n)\dot{\theta}_n + g(\theta_n) + p(F_d) \qquad 2.8$$

where, $I(\theta_n)$ is the inertial matrix, $c(\theta_n, \dot{\theta}_n)$ represents the coupling between Coriolis and centrifugal forces, $g(\theta_n)$ is the gravitational vector, and $p(F_d)$ represents the perturbation forces due to interaction with the external load. This dynamic model is the same as that used in the study of robotics (Craig, 1989). Given the nominal trajectory, θ_n, the joint torques T_n can be computed. Equation 2.8 represents the inverse limb dynamics component of the feed forward controller. The forward version of this equation could also be used in the forward limb dynamics block as part of the design process.

Muscle activation dynamics pose a more fundamental problem. The primary impediment to the development of muscle activation dynamics models is that muscle is a highly nonlinear, time-varying system. Add to this the lack of fundamental understanding that prevents development of an *a priori* model from first principles (Kearney 1990), and the problem becomes even more difficult. Empirical system models based on the force-velocity, and length tension relationships can be developed to cope with the problem. For example, Lan (1990) used a discrete time parametric model of muscle dynamics which is the product of three factors: a linear autoregressive model of activation dynamics, a linear approximation of length-tension properties, and a piecewise linear function force-velocity model (presented in greater detail by Bernotas, 1986, 1987). This was deemed successful by Bernotas, but such a model considers only the dynamic properties of the muscle activation.

A potential enhancement to such modeling techniques comes in the recognition that force-velocity, and length-tension are not, by their nature, dynamic, and do not capture all the complexities of muscle in vivo — a system with significant dynamic components, and properties more complex than those modeled by the force-velocity and length-tension models (as discussed in section 2.4). Further, the parametric model presented by Bernotas can only capture time-varying system properties by implementation of an adaptive parametric identification scheme (discussed section 3.1.1).

The use of the force-velocity, and length tension models, along with adaptive parameter estimation was a practical approach — perhaps the only logical approach — given the constraints of application, but fundamental questions remain concerning the dynamic properties of muscle, in vivo, subject to electrical stimulation. This is a motivation for the work presented in this thesis — the application of time-varying system identification tools to gain a better understanding of the dynamic mechanical properties of electrically stimulated muscle.

3 Theory

3.1 Time-Varying System Identification

Section 2.4 alluded to the classic system identification problem, identification of the transfer function H(s):

$$H(s) = \frac{Y(s)}{X(s)} \qquad 3.2$$

Which transforms system input, x(t), to system output, y(t). In the time domain this is expressed as the convolution integral:

$$y(t) = \int_{-\infty}^{\infty} h(\tau)x(t-\tau)d\tau \qquad 3.3$$

Where $h(\tau)$ is the system's impulse response.

Given appropriate input-output records x(t) and y(t), equations 3.2 and 3.3 can be solved without making any *a priori* assumptions about the structure of the system. In solving equations 3.2 and 3.3 it is possible to solve for the function H(s) or $h(\tau)$ rather than identifying parameters of a system model developed *a priori*. This is important in neuromuscular control research because there are few guiding suppositions on which a tractable parametric system model can be developed from first principles.

Equation 3.2 can be solved directly using correlation techniques if x(t) has the following autocorrelation (Bendat and Piersol, 1986):

$$\int_{-\infty}^{\infty} x(t)x(t-\tau) = \Phi\delta(\tau) \qquad 3.4$$

Where $\delta(\tau)$ is the delta function ($\delta(\tau) = 1$ if $\tau = 0$, and $\delta(\tau) = 0$ if $\tau \neq 0$). In other words, the input must be uncorrelated white noise. If this condition cannot be met strictly, then a least square solution of equation 3.3 is possible (Hunter and Kearney, 1983a). The least square solution makes no formal demands on the input signal other than that the input must be rich enough to excite the system at the frequencies over which the system dynamics are to be identified. These solutions, and equation 3.3 itself, are, however, not appropriate for the study of time-varying systems. To study time-varying

systems new techniques must be employed. Four techniques are considered in the following section, these are: quasi-time-invariant methods, adaptive methods, ensemble methods, and finally functional expansion methods.

3.1.1 Survey of Theoretical Techniques

Quasi-Time-Invariant Methods

In one special case equation 3.3 can be applied to a system which varies in time, that is when the state of the system varies very slowly with respect the length of the system impulse response function, $h(\tau)$. In this case equation 3.3 can be expressed as (Hunter and Kearney, 1987):

$$y(t) = \int_{-\infty}^{\infty} h(\tau,\alpha)x(t-\tau)d\tau \qquad 3.5$$

Where α is the mean state (e.g. in a joint dynamics experiment α would be the mean activation level or joint position).

If α is permitted to vary continuously throughout an experiment (i.e. $\alpha = \alpha(t)$) then a series of piece-wise time-invariant analyses may be undertaken by solving equation 3.3 over a series of time intervals of length sufficient to permit solution of the equation. This is only valid if the variations in α are not significant over the chosen time interval. In general, the length of the time interval required to solve equation 3.3 is at least 2T (greater when noise rejection properties are considered), where T is the length of the system's impulse response function (Hunter and Kearney, 1987).

The compliance impulse response function for the human ankle joint is approximately T=200 ms in length, therefore, the time interval required to solve equation 3.3 is at least 2T=400 ms. If the quasi-time-invariant method is applied to human ankle joint dynamics, the system state must not change significantly over a time interval of 400 ms.

Muscle activation levels can vary over a wide range in less than 400 ms (Hunter and Kearney, 1987), and a single muscle twitch is completely finished in 400 ms (see figure 5.1), therefore, this technique is of no value in the identification of the variation of system dynamics during a event as fast as a single twitch.

Adaptive Methods

Adaptive methods are classified here into two related categories: recursive least square estimation, and Kalman filtering.

Recursive Least Square

The recursive least square method does just what its title states, it implements a least squares parameter estimator recursively with the added proviso that past input-output data is exponentially weighted so that parameter estimates are a function of only the most recent data and, therefore, are free to vary with time.

The recursive least square method (Ljung, 1987) operates on the linear system:

$$y(t) = \phi^T(t)\theta(t) \qquad 3.6$$

$$y(t) = \phi^T(t)\hat{\theta}+\varepsilon(t,\hat{\theta}) \qquad 3.7$$

where $\phi(t)$ is the input vector (or matrix), $y(t)$ is the output vector, $\theta(t)$ is the parameter vector, $\hat{\theta}(t)$ is the estimated parameter vector, and $\varepsilon(t,\hat{\theta})$ is the error in the output estimate given the parameter estimate $\hat{\theta}(t)$.

The recursive algorithm weights previous samples by a weighting function given by:

$$\beta(t,k)=\lambda^{t-k} \quad 0\le k\le t-1 \qquad 3.8$$

where $\beta(t,k)$ is the weighting function applied to calculate the parameter estimate at time t, weighting previous data at times k. So that, for example, the most recent datum ($k = t$) is weighted by $\beta(t,t) = 1$, the second most recent datum ($k = t-1$) is weighted by $\beta(t,t-1) = \lambda$, the third most recent datum ($k = t-2$) is weighted by $\beta(t,t-2) = \lambda^2$, etc. λ is termed the forgetting factor.

The parameter estimate, $\hat{\theta}$, which minimizes $\sum\varepsilon^2(t,\hat{\theta})$ is then given by (Ljung, 1987, equation 11.9):

$$\hat{\theta}(t+1)=\hat{\theta}(t)+R^{-1}(t)\phi(t)\left[y(t)-\phi^T\hat{\theta}(t)\right]$$
$$R(t)=\lambda R(t-1)+\phi^T(t)\hat{\theta}(t-1) \qquad 3.9$$

If the forgetting factor is $\lambda = 1$, then all previous data is weighted equally and the method becomes a regular least square method. If $\lambda < 1$ equation 3.8 decays

exponentially to zero and only the most recent data is reflected in the parameter estimate, $\hat{\theta}(t)$. Hence the method is capable of tracking variations in the model parameters.

The RLS method imposes constraints on the dynamics of the parameter variations which are related to the weighting function $\beta(t,k)$. Essentially, the state of the system cannot change significantly over the time period of previous samples which are heavily weighted by $\beta(t,k)$. Stability of equation 3.9 requires λ to be close to one; typical choices of λ are in the range 0.98 to 0.995. If λ is near one then the weighting function can be estimated with (Ljung, 1987):

$$\beta(t,k) = \lambda^{t-k} = e^{(t-k)\log\lambda} \approx e^{-(t-k)(1-\lambda)} \qquad 3.10$$

This means that measurements older than $1/(1-\lambda)$ samples are included in the parameter estimate with a weight that is $e^{-1} \approx 36\%$ of that of the most recent measurement. So that:

$$T_0 = \frac{1}{(1-\lambda)} \qquad 3.11$$

can be termed the *memory time constant* of the weighting function. If the state of the system remains approximately constant over T_0 samples, a reasoned choice of λ can be made from equation 3.11, or from the alternative point of view, if λ is selected before hand then the maximum allowable rate of parameter variation can be estimated. For example, if λ is 0.99 then $T_0 = 1/(1\text{-}0.99) = 100$ samples. If the sample rate is 200 Hz then the last 500 ms of measurements would be weighted significantly and, therefore, the system must remain relatively constant over this time interval.

A more formal discussion of tracking ability is provided by Gerencsér (1991), who has shown that the maximum tracking error of a slowly time-varying system is proportional to $\dot{S}^{1/3}$, and that the optimum value of λ is proportional to $\dot{S}^{2/3}$. Where $\dot{S}$ is the rate of change of the parameter variations (see equation 3.12). Formally, the slowly time-varying condition is satisfied if:

$$\sup_{t \geq 0} |\theta(t+1) - \theta(t)| \equiv \dot{S} < \infty \qquad 3.12$$

Gerencsér's results show that adaptive identification schemes will, unless there is no parameter variation (i.e. $\dot{S} = 0$), always have tracking error, and that the error increases as the rate of parameter variations increase.

Kalman Filter

A related technique, Kalman filtering estimates the optimal state vector of a state space system which is subject to input (process) and output (sensor) noise. By itself, this is not sufficient to perform system identification since only the state vector of the system is estimated, not the system that generated the state vector. However it is possible to formulate a state space system for which the state vector is comprised of the coefficients of a system model, and implement a Kalman filter which will estimate those model parameters.

Kalman (1960), developed a method for optimally (in a least squares sense) estimating and predicting the state of a discrete state space system given previous output measurements, and knowledge of the process and sensor noise covariance properties. The Kalman filter, as it is referred to today, is much lauded in modern control theory (Sorenson, 1970), and has application in system identification as well. The Kalman filter operates on the system:

$$\begin{aligned} x(k+1) &= F(k)x(k)+G(k)w(k) \\ y(k) &= H(k)x(k)+v(k) \end{aligned} \qquad 3.13$$

where k = 1, 2, ..., the output is y(k); w(k) and v(k) are zero mean random processes, with properties: $E[w(k)] = 0$, $E[v(k)] = 0$, and $E[w(k)w^T(j)] = Q(k)\delta_{kj}$, $E[v(k)v^T(j)] = R(k)\delta_{kj}$ (E denotes expected value).

The Kalman filter can provide the optimal state estimate, $\hat{x}(k)$, or the optimal one step prediction, $\hat{x}(k+1)$. In what follows here, only the estimator is considered. The optimal estimate of x(k) is (adapted from Sorenson, 1985):

$$\hat{x}(k) = \hat{x}(k-1)+K(k)[y(k)-H(k)\hat{x}(k-1)] \qquad 3.14$$

where K(k) is given by the recursive set:

$$\begin{aligned} K(k) &= P(k-1)H^T(k)\left[H(k)P(k-1)H^T(k)+R(k)\right]^{-1} \\ P(k) &= [I-K(k)H(k)]P(k-1) \end{aligned} \qquad 3.15$$

The Kalman filter can be adapted to estimate model parameters by forming a system:

$$\begin{aligned} \theta(t+1) &= \theta(t) \\ y(t) &= \phi^T(t)\theta(t)+v(t) \end{aligned} \qquad 3.16$$

which is simply equation 3.7 expressed in state space form, and equation 3.13 with $x(t) = \theta(t)$, $F(t) = I$, $H(t) = \phi^T(t)$, and $w(t) = 0$. The Kalman filter can then be computed from equations 3.14 and 3.15, and the estimated state will be the optimal parameter estimate $\hat{\theta}(t)$.

In this form, the Kalman filter cannot explicitly account for time-variations of $\hat{\theta}(t)$, in fact, Ljung (1987) shows that in this form the Kalman filter is equivalent to the RLS method with the forgetting factor set to $\lambda=1$, which is ordinary least square parameter estimation. It is possible, however, to account for parameter variations if a model of those variations is known *a priori* (i.e. $F \neq I$). In which case, with parameter noise also included, equation 3.16 becomes:

$$\begin{aligned} \theta(t+1) &= F(t)\theta(t) + w(t) \\ y(t) &= \phi^T(t)\theta(t) + v(t) \end{aligned} \qquad 3.17$$

This approach is used by Kitawaga and Gersch (1985), Moser and Graupe (1989), and Tsypkin and Bondarenko (1992), in an extended manner in which the parameter variations are modeled in a general way as a linear sum of the n past estimates. Their methods differ in some respects but have in essence the following approach.

The parameter estimate $\theta(t+1)$ is given by a linear combination of n past parameter estimates:

$$\theta(t+1) = A_1\theta(t) + A_2\theta(t-1) + \ldots + A_n\theta(t-n-1) \qquad 3.18$$

where A_1, ... A_n are constant nonsingular matrices which must be developed *a priori*. This expression may be recast as the matrix equation:

$$\begin{bmatrix} \theta(t+1) \\ \theta(t) \\ \theta(t-1) \\ \vdots \\ \theta(t-n) \end{bmatrix} = \begin{bmatrix} A_1 & A_2 & \cdots & \cdots & A_n \\ I & 0 & \cdots & \cdots & 0 \\ 0 & I & \cdots & \cdots & 0 \\ \vdots & & \ddots & & \vdots \\ 0 & \cdots & \cdots & I & 0 \end{bmatrix} \begin{bmatrix} \theta(t) \\ \theta(t-1) \\ \theta(t-2) \\ \vdots \\ \theta(t-n-1) \end{bmatrix} \qquad 3.19$$

where I is a unit matrix of the same dimension as θ. If a new parameter vector $\xi(t)$, and transition matrix A, are defined, then equation 3.19 becomes:

$$\xi(t+1) = A\xi(t) \qquad 3.20$$

The observation equation, 3.6, then becomes:

$$y(t) = \left[\phi^T(t) \quad 0 \quad \cdots \quad 0\right]\xi(t) \qquad 3.21$$

In the presence of noise in the parameter law, equation 3.20, and observation law, equation 3.21, an optimal time-varying parameter estimate would be determined by a Kalman filter, and the time variations in $\theta(t)$ could be followed.

In general, adaptive methods are capable of identifying time-varying systems but impose strict conditions on the system. In the RLS case the rate of change of the time variations is limited, and, in the case of the Kalman filter, it must be possible to model the parameter variations *a priori*. Both of these conditions are undesirable when one studies the neuromuscular system because large rapid changes in the state of the system can be expected, and because the underlying physiology is of sufficient complexity that *a priori* system models inevitable contain many parameters and function relations which cannot be measured directly (Kearney and Hunter, 1990).

Ensemble Methods

The limits imposed on the solution of equation 3.6 by adaptive methods can be overcome by collecting an ensemble of experimental input-output records to generate a set of realizations of equation 3.6 which can be solved simultaneously. The ensemble data consists of a large number of repetitions of the same response with a stochastic perturbation superimposed on top of each response to excite the system. The stochastic perturbation makes each response independent of the others, therefore, if an ensemble of m such input-output records is collected, equation 3.6 becomes a set of m independent equations:

$$y_k(t) = \phi_k^T(t)\theta(t) \qquad 3.22$$
$$k = 1, 2, \ldots m$$

At each point in time, t, equation 3.22 then becomes a matrix equation which can (as long as m is greater than the number of parameters) be solved for $\theta(t)$, in a least square sense, using matrix inversions techniques (Strang, 1980), or alternatively looked upon as an ARMA model and solved accordingly (Ljung, 1987). The ARMA approach was used by Bennet et al. (1990).

A parametric model is, however, not necessary for application of the ensemble technique. In fact, the more general nonparametric impulse response function, equation 3.3, is directly extensible to model time-varying linear behavior by simply making the

system's impulse response function, $h(\tau)$, vary with time (Lawrence et al., 1977; Soechting et al., 1981; Kearney et al., 1991):

$$y(t) = \int_{-\infty}^{\infty} h(t,\tau)x(t-\tau)d\tau \qquad 3.23$$

The time-varying transfer function would be (Bendat and Piersol, 1986):

$$H(t,s) = \frac{Y(s)}{X(s)} = \int h(t,\tau)e^{-j2\pi s\tau}d\tau \qquad 3.24$$

As is the case with equation 3.3, equation 3.23 can be solved directly using correlation techniques, if the input meets appropriate criteria, or in a more general way with a least square approach. The added requirement in the solution of equation 3.23, over the time-invariant case, is the necessity to use an ensemble of input-output realizations rather the single input-output realization sufficient to solve equation 3.3. Equation 3.23 can be solved if formulated as follows: begin by assuming h is zero outside the interval $\tau = -T, T$ so that,

$$y(t) = \int_{-T}^{T} h(t,\tau)x(t-\tau)d\tau \qquad 3.25$$

converting to finite discrete form,

$$y(i) = \Delta t \sum_{j=-n}^{n} h(i,j)x(i-j) \qquad 3.26$$

where $n = T/\Delta t$.

Equation 3.26, by itself, is underdetermined, but is solvable if a minimum of 2n+1 independent input-output realization are obtained such that:

$$y(i,k) = \Delta t \sum_{j=-n}^{n} h(i,j)x(i-j,k) \qquad 3.27$$

where k represents each realization of equation 3.26. Under these conditions equation 3.27 is solvable, and the time-varying convolution kernel, h(i,j), can be determined.

The important point of this section is not the solution of equation 3.27, but the recognition that this method of time-varying system identification imposes no

fundamental dynamic constraints on the identification — as do the quasi-time-invariant, and adaptive methods — and that a direct solution of equation 3.27 is, in fact, possible. For this reason, and because no constraints other than linearity are placed on the identification, the ensemble method has ideal properties for studying systems, such as the neuromuscular system, which are subject to rapid large variations in their dynamics properties, and for these reasons, was used in this study. A complete discussion of the ensemble method, and the solutions of equation 3.27, may be found in section 3.3.

Functional Expansion Methods

One further means of solving equation 3.23 is the functional expansion method of Marmarellis (1981, 1987). This method addresses the modeling of a class of time-varying systems, of which equation 3.23 is a member, through an extension of the Volterra-Wiener approach (Marmarelis, 1978) and the use of a modified cross-correlation technique that yields time-varying kernel estimates from single input-output data records.

In application to equation 3.23, the functional expansion method offers not a direct solution, but identifies a representation given by the finite expansion:

$$h(t,\tau) = \sum_{n=0}^{k} c_n(t)\beta_n(t) \qquad 3.28$$

where $\beta(t)$ is a set of orthogonal functions defined over the observation interval [0,R], and satisfies:

$$\frac{1}{R}\int_0^R \beta_m(t)\beta_n(t)d\tau = \delta(m,n) \qquad 3.29$$

A Fourier set, for example, will satisfy this condition. The object of the identification task is $c_n(\tau)$, and is given by (Marmarelis, 1987):

$$\hat{c}_n(\tau) = \frac{1}{R}\int_0^R \beta_n(t)y(t)x(t-\tau)d\tau \qquad 3.30$$

Given this the kernel estimate is:

$$\hat{h}(t,\tau) = \sum_{n=0}^{k} \hat{c}_n(\tau)\beta_n(t) \qquad 3.31$$

Unlike the ensemble method this estimate can be made using single input-output records, but suffers from the need to select, *a priori*, a basis function, $\beta(t)$, which can describe the unknown time-varying impulse response function.

The ensemble method requires no model structure be selected *a priori*, and is preferable if the increased experimental demand of collecting an ensemble of input-output responses, rather than a single response, is tolerable.

3.1.2 Applications

Quasi-Time-Invariant Methods

An example of a situation for which quasi-time-invariant methods have been used is the identification of joint dynamics during muscle fatigue (Hunter and Kearney, 1983b). This study required subjects to maintain a constant 50% maximum voluntary contraction of the tibialis anterior muscle over an 80 second period while a random perturbation was applied about the ankle. Compliance impulse response functions were computed every 2.55 seconds so that changes in the mechanical properties of the joint (and therefore the fatiguing muscle) would be evident as changes in the impulse response function as the muscle fatigued. Fatigue onset at 50% maximum voluntary contraction occurred at a rate which was slow with respect to the 2.55 second window over which the compliance impulse response functions were estimated and the window was more than 10 times longer than the length of the same compliance impulse response functions (which were less than 200 ms). These are exactly the conditions (as discussed in section 3.1.1) under which a quasi-time-invariant analysis is appropriate. Based on this analysis Hunter and Kearney concluded that despite large increases in tibialis anterior EMG as the muscle fatigued, there were no corresponding significant changes in the ankle joint dynamics.

Adaptive Methods

Bernotas et al. (1986) and Chia et al. (1991) have used recursive least square methods to model the relationship between electrical stimulation intensity and force output of electrically stimulated muscle. These models consist of a parametric static nonlinearity followed by a second-order linear dynamic system, together expressed in a form appropriate for application of an exponentially weighted recursive least square algorithm. Such models are intended for real-time adaptive functional neuromuscular stimulation control systems such as described by Bernotas et al. (1987). Adaptive controllers, such as

that just described, represent the most common application of adaptive identification techniques but such techniques have also been applied directly to the study of time-varying joint dynamics.

Xu et al. (1991b, 1992) identified time-varying dynamics of the human elbow during simple unconstrained motions using exponentially weighted recursive least square methods. This work employed an actuation system capable of applying force perturbations without constraining the forearm (Xu, 1991a) and identified the dynamics of a second-order model:

$$I(t)\ddot{\theta}_p(t)+B(t)\dot{\theta}_p(t)+K(t)\theta_p(t)=\tau_p(t) \qquad 3.32$$

where I is inertia, B is damping, K is elastic stiffness, θ_p is perturbed joint angle, and τ_p is the perturbation torque. Xu et al. (1991a) manipulated this equation such that I(t), B(t), and K(t) could be identified using a recursive least square algorithm which does not require measurement of the higher order position derivatives $\ddot{\theta}_p(t)$, and $\dot{\theta}_p(t)$. The method, however, did not perform well when parameters varied faster than 0.5 Hz. The technique was modified to include explicit measurement of $\ddot{\theta}_p(t)$, and estimation of $\dot{\theta}_p(t)$ which permitted estimation of parameter variations up to 5 Hz, but experimental results revealed unpredictable variations in the inertial parameter which should have remained constant through time (Xu, 1992), thus calling the technique (or the validity of a second-order model) into question.

Ensemble Methods

The ensemble method has been applied by Bennet (1990,1993) to identify a parametric time-varying model of essentially the same system as described by Xu (1991a, 1992). In this work subjects were instructed to move their arm repeatedly between two targets while a force perturbation was applied to the forearm. Time-varying inertia, damping and elastic stiffness parameters of the elbow joint where identified by solving, at each point in time, a discrete version of equation 3.32 expressed in ensemble form (equation 3.22). The inertia parameter was found to be invariant with time (as would be expected), the elastic stiffness was found to increase at points of highest acceleration (at the targets). The damping, however, presented no repeatable trend across subjects. Similar studies were conducted out by Lacquaniti et al. (1981, 1993). The authors do not discuss how much of the measured data is accounted for by the identified model.

Nonparametric ensemble methods have been applied to joint dynamics by Soechting et al. (1981), MacNeil et al. (1992), and Kirsch and Kearney (1991).

Soechting et al. (1981) examined the properties of the forearm (elbow joint), and the biceps and triceps muscles under various conditions using a correlation based solution of equation 3.27. Torque perturbations were used to excite the system while subjects carried out tasks involving transitions from resist (i.e., resist the perturbation) to not resist, tracking a ramp position change, and "ballistic" movement tasks. In addition to identifying the elbow time-varying joint dynamics under these conditions, the authors also considered the time-varying activation dynamics of the biceps and triceps muscles by computing the time-varying impulse response function between torque and EMG.

MacNeil et al. (1992) and Kirsch and Kearney (1991, 1993) examined the time-varying properties of the ankle joint by applying position perturbations while subjects carried out a step change in voluntary activation (MacNeil, 1992), and the response due to an imposed movement (a stretch of triceps surae muscles). Both studies identified the time-varying stiffness impulse response function (TVIRF) of the ankle joint under these conditions. These papers, unlike Soechting et al. (1981), also present the variance of the output accounted for by the identified TVIRF's. MacNeil et al. (1989) found the stiffness TVIRF accounted for approximately 90% of the output variance before, during, and after, the step change in activation. Kirsch and Kearney (1991) found the stiffness TVIRF accounted for was 75-80% before the stretch, but dropped to 50-60% after the stretch.

3.2 Interpreting the Time-Varying Convolution Integral

Among the possible time-varying system identification approaches offered in section 3.1 the one considered most appropriate for the identification of the large rapid variations expected during a twitch, was the ensemble method which provides a solution of the time-varying convolution integral:

$$y(t) = \int_{-\infty}^{\infty} h(t,\tau)x(t-\tau)d\tau \qquad 3.33$$

Equation 3.33 is the most direct —but as shall be demonstrated, not the only— time-varying extension of the standard time-invariant convolution integral:

weighting function must be a mirror image of the impulse response. In either case, both operations are neatly described by equation 3.34 as long as h does not vary with time.

This distinction between impulse response function and weighting function represent nothing new in the theory of time-invariant systems, and is normally not even noted in texts, but is an important consideration if equation 3.34 is modified to include time-varying dynamics.

If a system's response to an impulse varies with time, then the component of the output at time t due to excitation by an impulse applied at time t_1=t-τ will be $h_{imp}(t_1,\tau)x(t_1) = h_{imp}(t-\tau,\tau)x(t-\tau)$, and the total output at time t will be the sum of excitation over all times τ, which is expressed by the convolution integral:

$$y(t) = \int_{-\infty}^{\infty} h_{imp}(t-\tau,\tau)x(t-\tau)d\tau \qquad 3.35$$

If the weighting function varies with output time, t, then the component of the output at time t due to excitation applied at time t_1=t-τ will be $h(t,\tau)x(t_1) = h(t,\tau)x(t-\tau)$ and the output at time t will be the weighted sum of input over all times τ. This leads to equation 3.33.

The convolution kernel of equation 3.33 is referred to as the time-varying weighting function (TVWF) and is symbolized as "h", or for the purposes of the following discussion, as "h_w". The convolution kernel of equation 3.35 is referred to as the time-varying impulse response function (TVIRF) and is symbolized here as "h_{imp}".

The time-varying impulse response function versus the time-varying weighting function.

Although h_w and h_{imp} are not equivalent, there is a relationship between the two.

Equations 3.33 and 3.35 perform the same operation (convolution) on the same input, x(t), to generate the same output, y(t), therefore, the convolution kernel parts of the two integrands must be equivalent:

$$h_{imp}(t-\tau,\tau) = h_w(t,\tau) \qquad 3.36$$

Applying the variable transformation, $t_1 = t-\tau$:

$$h_{imp}(t_1,\tau) = h_w(t_1+\tau,\tau) \qquad 3.37$$

So that given the TVWF, h_w, the system's TVIRF, h_{imp}, at any time t_1 lies along the TFWF diagonal: $h_w(t_1+\tau,\tau)$.

To understand the relationship between h_w and h_{imp} consider what happens if the state of the system is frozen (i.e. stops varying with time) at time t_1. In that case the impulse response at all times after t_1 is the same as the impulse response at time t_1. If all time after time t_1 is denoted by $t_1+\tau$ then (with prime indicating the state if the system is frozen):

$$h'_{imp}(t_1,\tau) = h'_{imp}(t_1+\tau,\tau) \qquad 3.38$$

Which implies (under the same conditions):

$$h'_{imp}(t_1+\tau,\tau) = h'_w(t_1+\tau,\tau) \qquad 3.39$$

or,

$$h'_{imp}(t,\tau) = h'_w(t,\tau) \qquad 3.40$$

Equation 3.40 formalizes what would be expected if the state of the system was frozen — that the TVIRF and the TVWF would be equivalent since the system would no longer be varying through time. Equation 3.40 also provides a formal means of interpreting the TVWF. That is, at each point in time t, the weighting function, $h_w(t)$, is equivalent to the impulse response of a time-invariant system with the instantaneous properties of the time-varying system at time t.

Note, this short section has made explicit distinction between weighting function, and impulse response function; this was done to ensure clarity in the argument. Generally, however, the term *time-varying impulse response function* is used generically, without regard for the distinction drawn here. This is the case in the rest of this thesis. The context of the presentation should be examined if the reader wishes to distinguish between time-varying weighting function and time-varying impulse response function as described here (i.e. results derived from equation 3.34 are weighting functions, results derived from equation 3.35 are impulse response functions, the results presented later in this thesis are derived from equation 3.34)

3.3 Solution of the Time-Varying Convolution Integral

Section 3.1 (*ensemble methods*) discussed the conditions under which the time-varying convolution integral could be solved directly. The solution is based on collecting an ensemble of input-output trials (k = 1, 2, ... m) sufficient in number to solve the set of simultaneous equations represented by equation 3.27, repeated here:

$$y(i,k) = \Delta t \sum_{j=-n}^{n} h(i,j)x(i-j,k) \qquad 3.41$$

Given an ensemble of input-output data the time-varying convolution integral can be solved using variations on the correlation and matrix inversion techniques used to solve the time-invariant convolution integral.

3.3.1 Correlation Based Solution

The correlation based solution proceeds as follows, beginning with equation 3.41 (for clarity, the explicit sum bounds are excluded):

$$y(i,k) = \Delta t \sum_{j} h(i,j)x(i-j,k) \qquad 3.42$$

for an ensemble of realizations, k = 1, 2, ..., m.

If h was not time-varying (with respect to discrete time i), familiar correlation techniques could be used to solve this equation. In the time-varying case, a variation of this technique can be used to solve for h. To begin let the input be:

$$x(i,k) = X(i+k) \qquad 3.43$$

therefore, each realization the input, x(i,k), is X shifted forward k samples.

Now multiply 3.42 by x(i-k,k)

$$y(i,k)x(i-k,k) = \Delta t \sum_{j} h(i,j)x(i-j,k)x(i-k,k) \qquad 3.44$$

and sum over k, then substitute equation 3.43 and simplify:

$$\sum_{k} y(i,k)x(i-k,k) = \Delta t \sum_{j} h(i,j) \sum_{k} x(i-j,k)x(i-k,k) \qquad 3.45$$

$$\sum_k y(i,k)X(i-k+k) = \Delta t \sum_j h(i,j) \sum_k X(i-j+k)X(i-k+k) \qquad 3.46$$

$$\sum_k y(i,k)X(i) = \Delta t \sum_j h(i,j) \sum_k X(i-j+k)X(i) \qquad 3.47$$

If X is a zero mean random signal then the following is true:

$$\sum_k X(i-j+k)X(i) = \Phi\delta(k-j) \qquad 3.48$$

where $\delta(k-j)$ is the delta function and equals one when k=j, zero otherwise. Substituting equation 3.48 into equation 3.47 gives:

$$\sum_k y(i,k)X(i) = \Delta t \sum_j h(i,j)\Phi\delta(k-j) \qquad 3.49$$

Because $\delta(k-j)$ has a non-zero value only when j=k:

$$\sum_k y(i,k)X(i) = \Delta t\,\Phi h(i,k) \qquad 3.50$$

Thus the final result is:

$$h(i,k) = \frac{1}{\Delta t\,\Phi} \sum_k y(i,k)X(i) \qquad 3.51$$

Suitability of the correlation approach.

As evidenced by the results of Soechting et al. (1981), and Lawrence and Dawson (1977), the correlation based solution offers a viable solution of the TVWF but does impose restrictions on the input signal. These are: i) the input must be uncorrelated white noise, and ii) equation 3.43 must hold from one input to the next. Requirement (i) does not seem unduly harsh given that all the identification methods discussed so far depend on some sort of random signal; it is, however, very difficult in practice to generate a signal which is perfectly white (Kearney and Hunter, 1990). Requirement (ii) can present a considerable problem because it requires the physical response under study to be synchronized in some way with the input signal. This imposes experimental timing requirements which may, in practice, be difficult to meet. Fortunately, the pseudo-inverse solution makes no formal restrictions on the "whiteness" of the test signal, and makes no demands of the nature of requirement (ii).

3.3.2 Pseudo-inverse Solution

The pseudo inverse solution proceeds by forming a matrix equation from equation 3.41, given input-output realizations k = 1, 2, ... m. Equation 3.41 is recast in matrix form:

$$\begin{aligned} y(i,1) &= \Delta t\,[h(i,-n)\,x(i+n,1) + \ldots + h(i,n)\,x(i-n,1)] \\ &\vdots \\ y(i,m) &= \Delta t\,[h(i,-n)\,x(i+n,m) + \ldots + h(i,n)\,x(i-n,m)] \end{aligned} \qquad 3.52$$

$$Y_i = \Delta t\, X_i\, H_i \qquad 3.53$$

Where Y_i is a m by 1 vector, X_i is an m by 2n+1, and H_i is a 2n+1 by 1 vector. The problem now becomes the solution of equation 3.53. This is a standard problem in matrix algebra, the solution of which proceeds as follows. First convert to the simpler notation:

$$Ax = b \qquad 3.54$$

where $A = \Delta t\, X_i$, $b = Y_i$, and $x = H_i$.

If m = 2n+1 (i.e., the number of realizations, m, equals the number of points in the impulse response function, 2n+1) then the solution is the ordinary matrix inverse, $x = A^{-1}b$. This condition, however, will only yield the correct solution if the system is noise free. When m = 2n+1, b is necessarily in the column space of A and the solution, x, has no freedom to reject noise because it lies also in the column space of A. If m > 2n+1, Ax must still be in the column space of A, but b is free to lie outside that space, and a solution can be developed to minimize the error |Ax - b|. All responses which can be modeled by A (i.e. the system model) lie in column space. When b lies outside of this space it is because: i) b contains random noise which naturally cannot be modeled, ii) b contains components due to unmodeled behavior, or iii) b contains components to inputs which have not been considered.

From a geometric perspective, the error function $\varepsilon = |Ax - b|$ is the distance between b and the solution vector Ax. This function is minimum when Ax is the orthogonal projection of b into the column space of A, which means Ax - b is perpendicular to the column space of A. Given a vector Ay (where y is a 2n+1 by 1 vector) which represents any vector in the column space of A, then Ax - b will be perpendicular to Ay when the

dot product between the two is zero. This is expressed in equation 3.55, which simplifies to equation 3.57.

$$(Ay)^T(Ax - b) = 0 \qquad 3.55$$

$$y^TA^T(Ax - b) = 0 \qquad 3.56$$

$$y^T(A^TAx - A^Tb) = 0 \qquad 3.57$$

A nontrivial solution of equation 3.57 requires $y \neq 0$, therefore, the vector, x, which minimizes $\varepsilon = |Ax - b|$ is the solution of:

$$A^TAx - A^Tb = 0 \qquad 3.58$$

or,

$$x = (A^TA)^{-1}A^Tb \qquad 3.59$$

The expression $(A^TA)^{-1}A^T$ is termed the pseudo-inverse of A, and notated:

$$A^+ = (A^TA)^{-1}A^T \qquad 3.60$$

such that:

$$x = A^+b \qquad 3.61$$

Singular value decomposition applied to the pseudo-inverse.

This solution is a useful theoretical result, but suffers numerically due to the extreme rank instability of A^TA. (That is to say, the existence of $(A^TA)^{-1}$ is not guaranteed.) The singular value decomposition remedies this (Strang, 1980). Singular value decomposition decomposes A into:

$$A = Q_1 \Sigma Q_2^T \qquad 3.62$$

Where Q_1 is a m x m orthogonal matrix, and Q_2 is a n x n orthogonal matrix, and Σ is a m x n matrix which has special structure and properties, discussed further on, which remedy the rank instability problem. Substitute equation 3.62, into equation 3.60 to obtain:

$$A^+ = \left((Q_1 \Sigma Q_2^T)^T \; Q_1 \Sigma Q_2^T\right)^{-1} \left(Q_1 \Sigma Q_2^T\right)^T \qquad 3.63$$

Which reduces, due to the orthogonal properties of Q_1 and Q_2, to:

$$A^+ = Q_2 \left(\Sigma^T \Sigma\right)^{-1} \Sigma^T Q_1^T \qquad 3.64$$

$$A^+ = Q_2 \Sigma^+ Q_1^T \qquad 3.65$$

Σ^+, the pseudo-inverse of Σ, is a n x m diagonal matrix of inverse singular values (Golub, 1983):

$$\Sigma^+ = \text{diag}(\mu_i^{-1}, \ldots, \mu_r^{-1}, 0, \ldots, 0) \quad \in \quad \Re^{n \times m} \qquad 3.66$$

where r is the rank A.

In practice, this form of the pseudo-inverse is preferable to equation 3.60 because the rank deficiencies which arise due to dependent columns of A^TA become evident as very small singular values μ_i. These singular values can be set to zero before inverting the singular value matrix so that the pseudo-inverse remains stable (Strang, 1980).

The least square solution to equation 3.41 at discrete time i is finally:

$$H_i = \frac{1}{\Delta t} X_i^+ Y_i \qquad 3.67$$

Suitability of the pseudo-inverse approach.

The pseudo-inverse solution has the essential favorable property that it makes none of the strict requirements on the input signal, or experimental protocol, that the correlation based solution does. The trade off for these relaxed experimental requirements are the substantial computational requirements. When implementing an experimental protocol the relaxed experimental requirements of the pseudo-inverse solution far outweigh any computational disadvantage. For this reason, the pseudo-inverse approach has been selected for the analysis presented in the following sections.

4 Experimental Procedures and Analysis

4.1 Paradigm

The experiments involved fixing the subject's left foot to a mechanical actuator which applied a small position perturbation while, at the same time, an electrically stimulated twitch was elicited from the triceps-surae muscle group. The electric stimulus was applied using a surface electrode held underneath the knee. The stimulus was applied at random intervals so that subjects could not anticipate it. Ankle position, torque generated about the ankle, and soleus EMG where measured and recorded during each twitch response. Typically, several hundred responses were recorded for each subject.

To account for the dynamics of the actuator used to apply the position perturbation, a calibration test was performed by releasing the subjects foot from the actuator, and recording the torque generated by the actuator in response to the position perturbation alone. The resulting torque and position signals were then used to identify the dynamics of the actuator and fixation device so that their contribution to the recorded torque responses could be removed before the analysis.

4.2 Apparatus

Mechanical Actuator, Torque and Position Measurement

The actuator used to apply the position perturbation was a rotary hydraulic motor (Rotac 26R-2-1V, Ex-Cell-O Corp, Berne IN) controlled by a servo valve (Moog 73-233, Moog Inc, East Aurora, NY). The actuator was controlled by a simple proportional controller constructed from general purpose instrumentation amplifiers. Position was measured with a precision potentiometer (Beckman 6273-R5K, Beckman Industrial, Fullerton, CA) with a maximum nonlinearity of ±0.2%. Torque was measured using a torque transducer (Lebow 2110-5K, Eaton Corp., Troy NY) with a stiffness of 10^5 Nm/rad and a maximum nonlinearity of ±0.1%. Details of this actuator are described by Kearney (1983).

The position perturbation signal was a 200 Hz pseudo random binary sequence (PRBS) low pass filtered at 80 Hz with an 8 pole constant delay filter. The perturbation

signal was approximately 3000 samples (i.e. 15 seconds) long and replayed cyclically throughout the experiment.

The position and torque signals were conditioned and amplified with general purpose instrumentation amplifiers, low-pass (anti-alias) filtered at 250 Hz with 8-pole constant delay filters, then sampled at 2000 Hz with 16 bit analog to digital converters with a range of ±10 V. The analog to digital converter ran continuously and was triggered, by the same source which triggered the stimulator. One second of pre trigger data and 1.5 seconds of post-trigger data were collected for each response. Time zero (i.e. the time domain origin) of the torque and position signals was defined to be the time of application of the electrical stimulation.

Electrical Stimulation and EMG Measurement

Electrical stimulation was applied beneath the knee using a custom made ball electrode which was attached to a custom made gimbal which allowed the electrode to be positioned freely under the knee. The gimbal included a locking mechanism so that once it was positioned it remained that way for the duration of the experiment. The gimbal was attached to a half cast which was strapped to the subject's upper leg. A 4.5×4 cm carbon rubber ground electrode was placed on the subject's upper leg just above the patella.

The electric stimulus was a constant voltage 500 μs monophasic square pulse. The stimulation output current was limited to a maximum of 50 mA. Responses were monitored by a custom made EMG amplifier which included a special input stage designed to block the electrical stimulation transient. EMG was monitored throughout each experiment to ensure the stimulus response remained unchanged. A stimulus of sufficient amplitude to elicit a large M wave and a small H wave was chosen so that the response was due mainly to direct activation of the triceps surae muscles with little reflex activation. The stimulus amplitude required to achieve this varied from subject to subject but was typically in the range of 40-60 volts.

Stimuli were applied at random intervals based on a Poisson distribution with a minimum inter-pulse interval of 10 seconds, a maximum inter-pulse interval of 20 seconds, and an average inter-pulse interval of 13.33 seconds.

The electrical stimulator was custom made, but followed the design of a commercially available stimulator (Digitimer DS2).

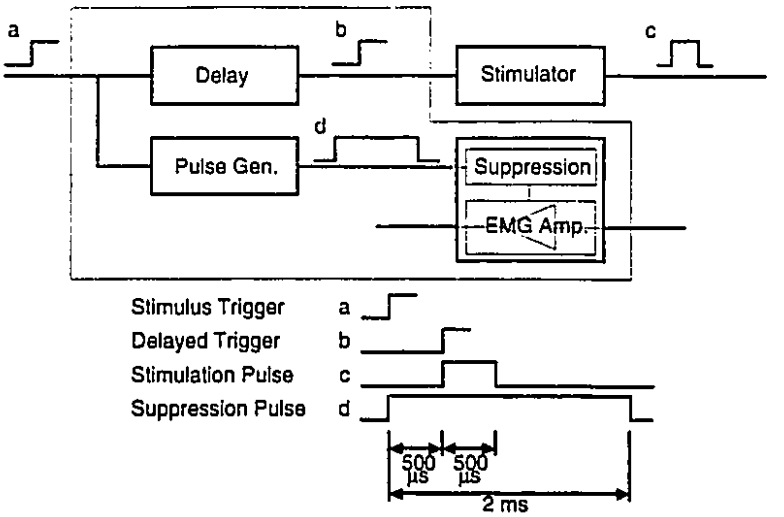

Figure 4.1. Block diagram of the artifact suppression circuit used to record EMG during electrical stimulation. The stimulator trigger (a) is delayed by 500 µs and passed on to the stimulator trigger input (b), at the same time a 2 ms pulse (d) is generated to activate the EMG amplifier suppression circuit. The stimulation pulse (c) goes directly to the electrode.

Response to the stimulation was monitored by recording EMG of the soleus muscle. EMG was measured by placing two Ag/AgCl electrodes (Electrotrace, Jason, Huntington Beach, CA) on the belly of the soleus muscle, parallel to the muscle fibers, in a bipolar configuration. A reference electrode (of the same type) was placed directly over the tibia.

The EMG amplifier was custom made and consisted of an instrumentation amplifier (Analog Devices AD625), a passive single pole 1 Hz high pass filter, a stimulus artifact suppression circuit, and an isolation amplifier. The artifact suppression circuit was designed to isolate, and hold the state of, the 1 Hz high pass filter for a short interval which overlapped the stimulus pulse. Without this, the artifact caused by excitation of the 1 Hz filter would have overwhelmed the EMG signal (less than 50 ms to the end of the H wave). The suppression circuit was set to come on 500 µs before application of the stimulation pulse (which itself was 500 µs long), and to remain on for 2 ms. The M wave appears approximately 5 ms after the stimulus is applied, therefore, the suppression circuit did not interfere with the EMG measurement. Figure 4.1 shows schematically how the artifact suppresser synchronized activation of the EMG artifact suppression circuit and the onset of the actual stimulation pulse.

The EMG signal was anti-alias filtered at 250 Hz with an 8-pole constant delay low-pass filter and sampled at 2000 Hz with a 16 bit analog to digital converter with a range of ±10 V.

Experimental Control and Data Collection

The position perturbation, and stimulus trigger were both generated by an IEEE488 programmable D/A converter. The trigger signal was passed to the electrical stimulator and to an IEEE488 programmable A/D converter which was configured to commence data collection on that signal. The A/D converter was configured to save one second of pre-trigger samples, and to continue sampling data for another 1.5 seconds. When sampling was complete, the A/D converter interrupted a general purpose laboratory computer which acted as the IEEE488 bus controller. This computer downloaded the position, torque, and EMG data from the A/D converter, and saved them for later processing. The laboratory computer played no role in controlling the experiment other than initial programming of the instruments, and downloading data from the A/D converter.

4.3 Analysis

The raw data collected for each experiment consisted of an ensemble of position and torque input-output records and calibration data consisting of a single input-output record. Before applying equation 3.67 to identify the time-varying dynamics of the joint, there are several preprocessing steps which were applied to the data. These are described in the next section. After the time-varying joint dynamics were computed, several post-processing steps were applied to generate results which are useful for interpretation.

4.3.1 Pre-processing

Resampling

The raw data was collected at 2000 Hz, but it proved not necessary, or wise, to perform the analysis at such a high sampling rate. The number of operations required to compute the pseudo-inverse (using singular value decomposition) increases exponentially with the sampling rate of the data, therefore, it was desirable to use the lowest possible sampling rate for the calculations. Proper selection of sampling rate at which to perform

the analysis requires consideration of the power spectrum of the input signal used to excite the system:

The position perturbation was a 200 Hz pseudo-random binary perturbation (PRBS) which was low pass filtered at 80 Hz, and used to drive a position servo which had a bandwidth of approximately 125 Hz. Therefore, there was no useful information in the raw data at frequencies much greater than 80 Hz, and even less beyond 125 Hz. There is little to be gained, therefore, by performing the computation at sampling rates which reflect dynamics at frequencies significantly higher than this. In fact, going well beyond the power bandwidth of the input only introduces noise which can have a detrimental effect on the identification.

The data is resampled, or *decimated* by extracting every n'th point from the raw data, where n is the *decimation ratio*. To avoid frequency aliasing the data must be numerically filtered to remove power above the Nyquist frequency of the decimated data. In this case the raw data was filtered at 0.8 times the Nyquist frequency using an 8'th order Chebyshev type 1 digital filter with 0.05 decibels of ripple in the pass band, and the data was filtered in both directions to give a result with zero phase shift. A decimation ratio of 8 was selected to give a new sampling rate of 250 Hz. This decimated signal therefore will have a bandwidth 0.8 times the Nyquist rate, or 0.8*(250/2) = 100 Hz, which is appropriate given the input signal bandwidth (80 Hz). This decimation scheme was applied to all raw torque and position data.

The EMG signals were not resampled because they were not used as input to any analysis procedures, just as qualitative feedback about the state of the muscle during the twitch.

Removal of Actuator Dynamics

The measured torque is a combination of torque produced about the ankle joint by muscles acting at that joint, and torque produced by the actuator in response to the position perturbation:

$$Tq_{measured} = Tq_{ankle} + Tq_{actuator} \qquad 4.1$$

Note, because the actuator, ankle fixation device, and position sensor are mechanically linked by an extremely stiff link, the measured position, the position of the ankle, and position of the actuator are equal:

$$Pos_{measured} = Pos_{ankle} = Pos_{actuator} \qquad 4.2$$

The last step in each experiment was application of the same position perturbation used throughout the experiment but without the subject's foot attached to the actuator. These signals (called Tq_{cal} and Pos_{cal} for *calibration* torque and position) were used to identify the dynamics of the actuator. The dynamics of the actuator are described well by the standard linear time invariant model:

$$Tq_{cal} = \int_{-\infty}^{\infty} h_{act}(t,\tau) Pos_{cal}(t-\tau) d\tau \qquad 4.3$$

h_{act} can be determined using well known techniques (Hunter and Kearney, 1987), and the actuator's contribution to the measured torque can be removed to arrive at an estimate of the ankle torque:

$$Tq_{ankle}(t) = Tq_{measured}(t) - \int_{-\infty}^{\infty} h_{act}(t,\tau) Pos_{measured}(t-\tau) d\tau \qquad 4.4$$

The actual calculations were, of course, done using discrete mathematics.

Equation 4.4 was applied to each measured position-torque pair in the ensemble. All further analysis was done with Tq_{ankle}, and Pos_{ankle}.

Trial Selection

The ensemble method requires an ensemble of identical responses to some stimuli. In reality the ensemble will consist of a set of similar, but not identical responses. To improve the identification a subset of the experimental responses were selected to give a more uniform ensemble as input to the identification scheme.

There are two possible types of variations from one trial to the next. There can be variation in the onset of the response —an alignment error— which would be a very important consideration if the response was voluntary (Kearney et. al., 1991), and there can be variations in the magnitude and time course of the response.

In this case the response was an electrically stimulated twitch to which the subject responded involuntarily. The time domain of each torque and position record in the ensemble was fixed with respect to the time the electrically stimulus was applied; the instrumentation was configured such that the maximum error in establishing the time of

application of the stimulus could be no more than one sample (i.e. 1/(2000 Hz) = 500 μs) and on average would be half a sample, or just 250 μs. This is insignificant compared to the duration of the mechanical twitch response (which lasts approximately 500 ms) and is only a small fraction (approximately 1%) of the duration of the EMG response (which was complete in approximately 50 ms). Therefore, no further consideration need be paid to alignment of the position and torque records.

Small variations in the size and time course of the twitch from trial to trial do occur and the analysis benefits by selecting a subset of the most similar responses. The selection process was based on the torque response from 0.0 to 0.6 seconds (rather than the full length of the recorded torque signal which extends from -1.0 to 1.5 seconds) since the actual twitch response occurred over this interval.

The selection was done using the following algorithm:

```
set = ensemble of torque responses from 0.0 to 0.6 seconds
n = number of responses to select
m = number of responses in set
while (m > n)
        ensemble average = ensemble average of set
        for each response in set
                squared error = (ensemble average - response)^2
        end
        reject response with maximum squared error
        decrement m
end
```

This algorithm computes the ensemble average of the entire set, then rejects the response which deviates most from the average. This process is applied repeatedly until a predetermined number of responses remain.

Removal of the ensemble mean.

The ensemble method determines time-varying dynamics by relating input-output data across the ensemble as well as through time. This requires that the data be stationary across the ensemble, and through time (i.e. through the time course of the twitch, in this case). Because the ensemble consists of a set of like responses it is already stationary at each point in time across the ensemble. Indeed, this is a basic requirement of the ensemble method.

The responses are, however, not stationary through the time course of the twitch. The torque response changes drastically through time as the triceps surae muscles respond to the electrical stimulus. Successful application of equation 3.67 requires that this non stationary response due to the electrical stimulation be removed. This is done by subtracting the ensemble average from each response in the ensemble. This is done to both the position ensemble and the torque ensemble. This procedure is essential to successfully identify the dynamics of the system. Removing the ensemble mean effectively reduces the system from a two input single output (input: position perturbation and electrical stimulus; output: sum of torque due to perturbation and stimulus), to a single input single output system (input: position perturbation; output: perturbed torque response).

4.3.2 Post-processing

After the preprocessing steps were applied to the raw data, a time-varying stiffness impulse response function (TVSIRF) was computed using equation 3.67. The first step in analyzing this result was to compute a measure of how well the TVSIRF modeled the input-output data.

Variance Accounted For

The impulse response function computed with equation 3.67 is a least square solution of $Y_i = \Delta t\, X_i\, H_i$ (equation 3.53). The solution to equation 3.53 is the component of Y_i (i.e. - the output, in this case torque) which lies in the column domain of X_i (i.e. - the input, in this case position). The vector $\Delta t\, X_i\, H_i$ is the component of Y_i which lies in the column domain of X_i, if H_i is computed using equation 3.67. If Y_i lies outside the column domain of X_i there will no vector H_i which perfectly models the system. This is a constraint of the linear model chosen to represent the system's dynamics. As stated before, there are several things which will cause Y_i to lie outside the column domain of X_i, these include: noise, nonlinear effects, and unmodeled inputs. The magnitude of the error vector containing these effects is $|Y_i - \Delta t\, X_i\, H_i|$. The accuracy of the model can thus be assessed at each point in time by comparing the magnitude of the error vector with the magnitude of Y_i itself. This is done by computing variance accounted for, at discrete time i, using the equation:

$$VAF_i = \left[1 - \frac{|Y_i - \Delta t\, X_i\, H_i|^2}{|Y_i|^2}\right] \qquad 4.5$$

This compares the square of the vector magnitudes rather than just the magnitudes, and is consistent with the definition of VAF used to assess time invariant system models, with the exception that the estimated and actual outputs are compared across the ensemble rather than through time.

If the system is noise free and perfectly modeled by a time-varying linear model the VAF will be one. If no element of the system can be modeled by a time-varying linear system the VAF will be zero (i.e. Y_i is perpendicular to the column space of X_i).

Smoothing

The TVSIRF solution usually contains a large magnitude noise component at the Nyquist frequency which must be removed by a filtering operation. This noise results because the solution attempts to model high frequency noise present in the input-output ensembles. Since there is not sufficient power at the high end of the spectrum for system identification, the solution tends to be dominated by incoherent, large magnitude, high frequency noise. These components of the solution must be explicitly removed by individually filtering each impulse response function in the ensemble.

The filter used to remove this noise was a two sided, three point smoothing filter. This operation does not completely rid the impulse response functions of the undesirable noise component, but does decrease its magnitude to the point where it does not dominate the impulse response. The operation does not introduce any phase shift into the stiffness IRF's (because the smoothing filter is two sided).

The smoothing operation was necessary but introduced one problem, which had to be overcome. A stiffness impulse response function for a system which has no delay should, theoretically, have just three non-zero points. These are at discrete lag time zero, and at discrete lag times -1, and 1. Non-zero values outside these three represent a delay in the system, filtering of the impulse response, or are simple noise. The problem caused by the averaging filter is the introduction of filtering transients which amplify noise at both ends of the stiffness impulse response. These are highly undesirable and must be removed. One plausible means of removing the transients is to simple truncate the stiffness impulse responses. The problem with simple truncation is that the end values of the impulse response after truncation may still have random non-zero values. A better approach, which forces the transients to zero, without disturbing the important information around lag zero, is to multiply the impulse response by a windowing function which is zero at the

ends and one in the middle. A logical choice, given that the impulse response function is 2n+1 points long, is the Hamming function:

$$\text{hamming}(i) = \frac{1}{2} - \frac{1}{2}\cos(2\pi\frac{(i+n)}{2n})$$
$$i = -n, -n+1, \ldots, n-1, n \qquad 4.6$$

Frequency Response — Average Low Frequency Stiffness

The TVSIRF quantitatively describes the dynamics of the system at each point in discrete time through the time course of the twitch. However, stiffness impulse response functions, while providing a sound mathematical description of a system's dynamics, do not yield well to direct interpretation. Part of this difficulty arises from the non-causal nature of the stiffness impulse response. Qualitative changes in the system's dynamics can be observed in the changing shape of the impulse response functions, but quantitative assessment requires further analysis of the TVSIRF itself. In short, the information in the impulse response functions must be expressed in a form more amiable to interpretation.

The simplest transformation which provides for easier interpretation is to compute the frequency domain transfer function as expressed in equation 3.24. Given the systems time-varying transfer function a Bode plot (i.e. magnitude and phase) is easily made. The transfer function magnitude is particularly easy to interpret because at low frequency it is representative of the elastic stiffness of the joint (keeping in mind the distinction, made in section 2.4, between dynamic and elastic stiffness). Therefore, an estimate of the time-variation in the elastic stiffness of the joint throughout the time course of the twitch can be had by averaging the transfer function magnitude at low frequency. This measure of elastic stiffness is termed *low frequency average stiffness* and is expressed formally by:

$$k_{low,i} = \frac{1}{\Omega}\int_0^{\Omega}\left|\frac{Tq_i(j\omega)}{Pos_i(j\omega)}\right|d\omega = \frac{1}{\Omega}\int_0^{\Omega}|H_i(j\omega)|d\omega \qquad 4.7$$

Where $H_i(j\omega)$ is the Fourier transform of the stiffness impulse response at discrete time i, and Ω is the frequency below which the transfer function magnitude is averaged.

To examine the relevance of low frequency average stiffness consider a second-order system which Kearney and Hunter (1990) have demonstrated to describes the dynamics

This simplifies to:

$$\frac{k_{low}}{k} = \frac{1}{\Omega}\int_0^{\Omega}\left[\left(1-\left(\frac{\omega}{\omega_n}\right)^2\right)^2+\left(2\zeta\frac{\omega}{\omega_n}\right)^2\right]^{\frac{1}{2}}d\omega \qquad 4.10$$

If the dimensionless quantities $\psi = \frac{\omega}{\omega_n}$, and $\Psi = \frac{\Omega}{\omega_n}$ are defined, then:

$$\frac{k_{low}}{k} = \frac{1}{\Psi}\int_0^{\Psi}\left[(1-\psi^2)^2+(2\zeta\psi)^2\right]^{\frac{1}{2}}d\psi \qquad 4.11$$

This relationship is shown in figure 4.2 for various values of ζ.

Figure 4.2 clearly shows the expected result: as $\Omega \to 0$, $k_{low} \to k$, and, as Ω increases k_{low} and k diverge. This figure proves useful in making a reasoned choice for Ω if estimates of the damping ratio, ζ, and the natural frequency, ω_n are available. This is considered further in the results section.

Fitting a Second-Order Model — Compliance IRF

The second-order parameters, k, ω_n, and ζ, are useful to consider not only because a second-order model has been shown to model time-invariant joint dynamics well, but also because such models are common in many fields of engineering and applied science and hence the parameters are widely understood and appreciated. To determine a set of time-varying second-order parameters a second-order impulse response function can be fit to each impulse response in the ensemble of time-varying impulse response functions.

The second-order parameters were estimated by fitting an analytic second-order impulse response function to each experimentally determined impulse response function in the time-varying ensemble. However, a time domain expression for the second-order stiffness impulse response function does not exist because the inverse Laplace transform of a function with more zeros than poles (i.e. — the second-order stiffness transfer function, equation 4.8) does not exist. The inverse Laplace transform of the compliance impulse response function does exist, however, and can be used to estimate the parameters of a second-order model. The expression for the second-order compliance impulse response function is:

$$\delta(t) = \begin{cases} \dfrac{\omega_n e^{-\zeta\omega_n t}}{k\sqrt{\zeta^2 - 1}} \sinh(\omega_n\sqrt{\zeta^2 - 1}\, t) & \zeta \neq 1 \\ \dfrac{\omega_n^2}{k} t e^{-\omega_n t} & \zeta = 1 \end{cases} \qquad 4.12$$

To estimate the parameters of this expression the experimentally determined stiffness impulse response functions must be individually inverted to get one sided compliance impulse response functions. This was done numerically by simply filtering a white noise input with each stiffness impulse response function to get an output signal, then identifying a time-invariant one sided filter between the output and input signals (i.e. output becomes input, and input becomes output). This result is referred to as a TVCIRF — time-varying compliance impulse response function.

The parameters of equation 4.12 were determined using the Levenberg-Marquardt non-linear least square parameter estimation technique (Press, 1986). This technique requires knowledge of the first partial derivatives, with respect to the parameters being estimated, of the equation under consideration. Analytic expressions for these derivatives, derived from equation 4.12, are presented in appendix one.

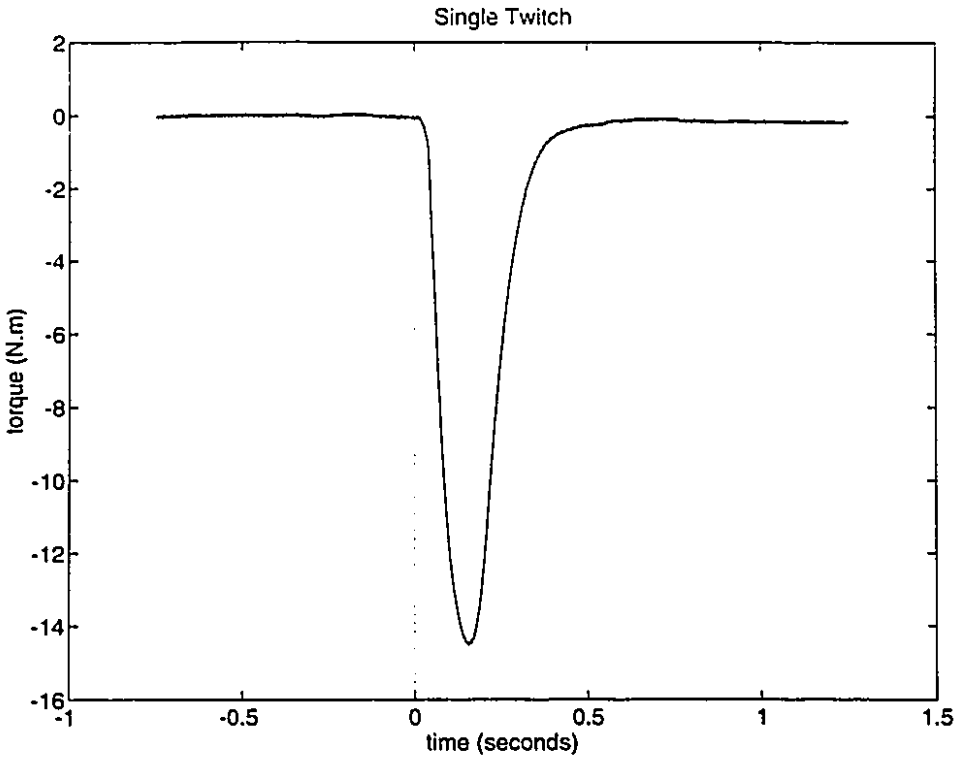

Figure 5.1. Plot of a torque generated about ankle by a single twitch of the triceps surae muscle group.

5 Results

The first group of figures in the this section, figures 5.1 to 5.7, are a collection of views of the raw data used to identify the time TVSIRF's. The TVSIRF's and plots relating directly to these follow in figures 5.8 to 5.14. The final set of results, figures 5.15 to 5.19, are the TVCIRF's and the resultant second parameter estimates.

The data presented here were collected from three male subjects in their mid-twenties with no known neuromuscular disorders. Data sets one, and two are from the same subject, but collected on two separate occasions. Data sets, three and four are from the other two subjects.

Single Twitch

Figure 5.1 presents a single twitch — the torque generated about the ankle joint by the triceps surae in response to stimulation of the anterior tibial nerve. The torque response peaks in approximately 125 ms and is over in 500 ms. Time zero is the time of

application of the stimulus. The small delay between time zero, and the onset of the twitch represents the time required for the action potential to travel down the anterior tibial nerve and depolarize the triceps surae muscles. Time zero has at most 500 μs, and on average 250 μs, of error (see section 4.3.1).

Perturbed Response

Figure 5.2 shows torque, position (perturbation), and EMG during a twitch. (Note, the EMG is on a different time scale.) The EMG recording clearly shows the motor activity occurring during the twitch. The first wave is a large M wave, begins at approximately 5 ms after application of the stimulus and is approximately 20 ms long; a small H-wave follows, it begins at approximately 35 ms and is approximately 10 ms long. The large M wave, in conjunction with a small H wave, indicates that the response was almost purely direct stimulation of the muscle (via the anterior tibial nerve) with little reflex response. The EMG was monitored throughout each experiment to ensure the effect of the electrical stimulation remained constant (i.e., maintained as presented in figure 5.2), but was not considered otherwise.

responses with which to continue the analysis. Fewer responses were collected in experiment one; therefore, no selection process was applied.

Table 5.1 also lists the resting position, and torque for each data set. The values represent the quiescent state of the system during the experiment. Note, the resting torque is a function of resting position only and represents the state of the passive structures of the joint and muscles. There is no active component in the resting torque; subjects were asked to maintain a relaxed state at all times during the experiments. This resting position and torque were removed from each torque and position record before any analysis was performed.

data set number	number of responses.	number of responses selected.	resting torque (N.m)	position perturbation standard. dev. (rad)
1	190	190	-6.3	1.75×10^{-3}
2	299	200	-7.0	2.75×10^{-3}
3	249	200	-7.7	3.00×10^{-3}
4	268	200	-10.5	4.25×10^{-3}

Table 5.1. Number of realizations of data for each experiment, the number of realization selected to perform the analysis (note, no selection process was applied to data set number one), the torque, and the standard deviation of the position perturbation.

The ensemble of torque and position records, for one data set, is shown in figure 5.6. This figure shows the ensemble mean plus and minus one standard deviation. The ensemble mean and standard deviation were computed across the data set at each point in time through the time course of the twitch. Solution of the time-varying convolution integral using the pseudo-inverse approach (section 3.3) requires the ensemble of input-output data be stationary through the course of the time-varying event. Figure 5.6 shows that this is clearly not the case during the twitch. The mean torque obviously changes substantially during the twitch; indeed, it is the variation in the state of the system during this non-stationarity which is of interest. The mean position also changes (to a much lesser extent) due to the finite stiffness of the position servo used to apply the position perturbation. Before proceeding, the ensemble mean must be removed from the torque and position data. The result of removing the ensemble mean from these signals is presented in figure 5.7.

Time-Varying Stiffness Impulse Response Functions

The pseudo-inverse identification procedure described in section 3.3.2 was applied to compute a time-varying stiffness IRF for each data set. Figures 5.8, 5.9, 5.10, and 5.11 present the results for each data set; each figure shows the complete time-varying stiffness IRF as a three dimensional plot. The individual impulse responses shown below these correspond to the instant the stimulus was applied (0.0 seconds), mid-response (0.25 seconds), and after full recovery (0.75).

In each case, the shape of the TVSIRF changes substantially between 0.0 and approximately 0.5 seconds through the time course of the twitch. This change in shape reflects the changing state of the system through the time course of the twitch. Before and after this interval the TVSIRF maintains a roughly constant shape reflecting the time-invariant state of the system before the application of the stimulus, and after full recovery.

In the absence of noise, a stiffness IRF has just three non-zero points. One positive non-zero point at lag zero, and one negative non-zero point on either size of lag zero. The magnitude of these points reflect the dynamic characteristics of the system. These features are easily distinguished in the individual IRF's with the exception that these IRF's are not noise free. The noise in the IRF's was reduced by multiplying each IRF by a Hamming window. The Hamming window forces the noise components to zero at the extents of the IRF (i.e., lag times -100 ms, and 100 ms) while having minimal affect in the vicinity of lag zero where the important dynamic information exists. Changes in the systems dynamics during the twitch are reflected in the magnitude of the IRF peaks approximately in the -20 to 20 ms region. The stiffness IRF's non-causal nature make direct interpretation difficult beyond simple recognition of changes in magnitude in this region.

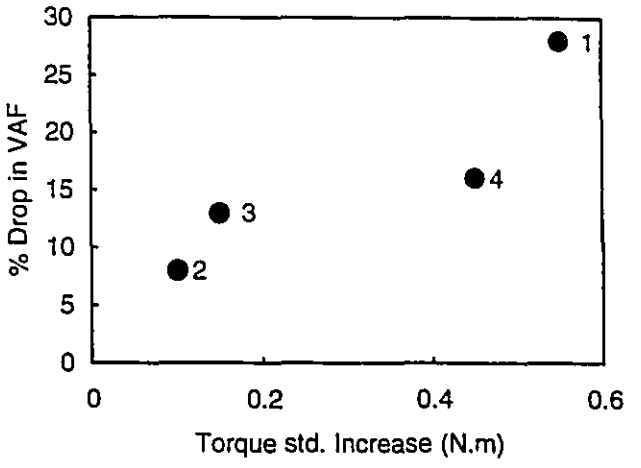

Figure 5.13. Relationship between the increase in standard deviation of the perturbed torque response, and the drop in VAF during the twitch. The linear trend suggests the drop in VAF is due to the inter-trial variability reflected by the increased standard deviation of the perturbed torque response.

5.2, and the increase in torque standard deviation is plotted in figure 5.13. The linear trend of the plot suggests the relationship expected if (i) is the primary cause for the drop in VAF.

data set number	torque std. before twitch (N.m).	max. torque std. during twitch (N.m)	increase in torque std. (N.m)	VAF drop during twitch (%)
1	0.80	1.35	0.55	28
2	1.40	1.50	0.10	8
3	1.35	1.50	0.15	13
4	1.55	2.0	0.45	16

Table 5.2. Standard deviation (std.) of perturbed torque before and during the twitch, their difference, and the magnitude of the drop in VAF during the twitch. Data in columns four, and five are plotted in figure 5.13.

$\frac{k_{low}}{k} \approx 1.0$, in other words, at rest the low frequency average stiffness will be approximately equal to the elastic stiffness. The elastic stiffness identified as part of the second-order analysis can, as a first approximation be expected to be close to the low frequency average stiffness.

Time-Varying Compliance Impulse Response Functions

The next step in the analysis was to invert the time-varying stiffness IRF's to obtain time-varying compliance IRF's. Recall, this step is necessary to proceed with the second-order parametric analysis. Also, the compliance IRF provides a representation of the dynamics which is much easier to interpret that the non-causal stiffness IRF's. The time-varying compliance IRF's are presented in figures 5.15 to 5.18.

As with the stiffness IRF's, these figures show, for each data set, the complete time-varying compliance IRF as a three dimensional plot. Below each of these are three individual impulse responses extracted from the time-varying compliance IRF at times 0.0, 0.25, and 0.75 seconds through the time course of the twitch. Again, these times correspond to the instant the stimulus was applied (0.0 seconds), mid-response (0.25 seconds), and after full recovery (0.75).

Again, qualitative changes in the systems dynamics are observable as changes in the shape of the time-varying compliance impulse response functions during the time course of the twitch. The individual compliance impulse response functions are easier to interpret in this case because they are causal. Note, that as in the stiffness case, the compliance impulse responses at 0.0 and 0.75 seconds are very similar, reflecting the constant state of the system before and after the twitch, but the compliance impulse responses at 0.25 seconds through the time course of the twitch are distinctly different. Before and after the twitch the IRF's have the characteristics of a second-order under-damped system; however, during the twitch (i.e., at 0.25 second) the IRF is no longer characteristic of a second-order under-damped system. The response at this time is more like an under-damped oscillatory response on top of a slower over damped component. This difference presents a key to determining what is happening to the state of the system during the twitch, and is explored in more detail in the next section.

Second-order Analysis

Figure 5.19 presents the results of fitting a second-order model to the time-varying compliance IRF's. The procedure estimated the natural frequency, damping ratio, and elastic stiffness (ω_n, ζ, and k). The inertia, and damping parameters were computed from ω_n, ζ, and k.

The second-order analysis was undertaken because it is known to successfully model joint dynamics under time-invariant conditions (Kearney and Hunter, 1990), and is, therefore, worth considering as a model for time-varying joint dynamics. First impressions of figure 5.19 may lead one to believe that the second-order model does not fair too badly. For example, the variance of the second-order impulse response (which indicates how closely the second-order parametric impulse response matches the nonparametric compliance impulse response at the each point in time) is reasonably high, dropping only to about 75% during the twitch. In addition the elastic stiffness rises during the twitch, as expected, and the resting elastic stiffness is very close to the resting low frequency stiffness. In these respects the second order model appears to successfully characterize the nonparametric results.

The second-order model does not fair well, however, when one examines how the inertia parameter varies. There is no reason to expect the inertia of the joint to vary during the time course of the twitch. Small fluctuations in the parameter estimates are not disturbing; but the inertia estimate should at least remain stationary. In each case the

6 Discussion

Facts and Theories

A system as complex as the neuromuscular system presents significant challenge to any identification scheme because it is both time-varying and nonlinear. The ensemble time-varying identification can successfully identify linear dynamics, and in the event the underlying system is nonlinear, can linearize the system about a fixed trajectory as it varies through time. The ensemble identification scheme does this well. By placing no constraint on the system other than that of linearity, and repeatability, the ensemble identification scheme gives a concise reliable description of the system's dynamics for the particular response under investigation. The next step in the identification process is one of interpretation; one of drawing conclusions about the significance of the result.

At this point it is natural to turn to some sort of parametric system model which will lead to a better understanding of the mechanisms underlying the observed response. This is a difficult step in the study of neuromuscular systems but is nevertheless important. As Wilkie (1954) wrote (from McMahon, 1984):

> *Facts and theories are natural enemies. A theory may succeed for a time in domesticating some facts, but sooner or later inevitably the facts revert to their predatory ways. Theories deserve our sympathy, for they are indispensable in the development of science. They systematize, exposing relationship between facts that seemed unrelated; they establish a scale of values among facts, showing one to be more important than another; they enable us to extrapolate from the known to the unknown, to predict the result of experiments not yet performed; and they suggest which new experiments may be worth attempting. However, theories are dangerous too, for they often function as blinkers instead of spectacles. Misplaced confidence in a theory can effectively prevent us from seeing facts as they really are.*

Second-order models have been used to describe joint dynamics because they facilitate the first of Wilkie's points; they *systematize* experimental results, turning that which is concise but difficult to interpret —in this case stiffness impulse response functions— into that which is concise but easy to interpret — the parameters of a model.

In this scenario, the facts are the nonparametric results, derived from raw data with as few biased constraints as possible, and the second-order model is the theory, potentially biased due to contrary assumptions. The nonparametric results are the facts used to verify the hypothesis that a second-order model is sufficient to characterize joint dynamics. Note, this is not to say that the second-order model is being considered as a definitive representation of joint dynamics and the associated underlying mechanisms,

rather, that it is simply an appropriate means of *characterizing* time-varying joint dynamics. However, while the second-order model has been successful in the study of time-invariant joint dynamics it is disappointing when applied to the study of time-varying joint dynamics.

MacNeil et al. (1992), and Kirsch et al. (1991, 1993) used the ensemble identification technique to study the time-varying dynamics of the ankle joint. MacNeil studied the dynamics during a voluntary change in activation level, while Kirsch examined changes during an imposed change in position. Both studies tried to fit second-order models to nonparametric results. MacNeil demonstrated that during the transient change in muscular activation the dynamics were not well modeled by a second-order system. Similarly, Kirsch et al. found that during a transient imposed stretch the dynamics of the joint were not well modeled by a second-order system.

Xu (1992), assumed a second-order model *a priori* and used an adaptive method to identify the second parameters describing the dynamics of the elbow joint during an isometric change in activation level, and during movement.. Xu's adaptive method was considered successful under time-invariant conditions, and in simulation was reported to successfully identify the parameters of second-order model when the variations where less that 5 Hz, yet with real data the results were considered inadequate. Xu found that the inertia parameter varied unpredictably, when it should have remained constant, thus raising questions about the suitability of the second-order model, or the success of the identification scheme. This leads one to believe that, again, the second-order model has failed under time-varying conditions.

Lacquaniti et al. (1981, 1993) used the ensemble correlation approach to study the dynamics of the human elbow joint during a voluntary change in activation level, and also used a second-order model to characterize the system's dynamics. Unfortunately, the prediction accuracy of the second-order model was not presented so the success of the second-order model could not be properly assessed. The same is true of Bennett (1990, 1993) who investigated elbow dynamics using a time-varying parametric identification scheme to estimate the parameters of a second-order model, but again the prediction accuracy of the second-order model was not presented so the validity of the second-order model could not be properly assessed. These two examples represent, perhaps, a case of (from Wilke, 1954): *"Misplaced confidence in a theory can effectively prevent us from seeing facts as they really are."*

The results of MacNeil et al. (1992), Kirsch et al. (1991, 1993), and Xu (1992), and the results presented here all indicate that the second-order model fails to *systematize* the facts uncovered by nonparametric studies of time-varying joint dynamics. Careful examination of the nonparametric results presented in this thesis do, however, give some clues as to what is missing from a model which aims to *systematize* the results of time-varying joint dynamics studies.

Facts to Guide Wayward Theories

To understand why a second-order model fails to model the time-varying joint dynamics it helps to examine, qualitatively, a single compliance impulse response extracted from the time-varying compliance impulse response function at a time when the state of the system was varying (which is also, of course, a time when the second-order model was not successful). Such an impulse response is shown in figure 6.1. Inspecting this impulse response leads to an obvious qualitative conclusion: the second-order model cannot characterize this impulse response because its shape is more complex than second-order. What it seems like, in fact, is an oscillatory response on top of a slower response. The oscillatory component could minimally be an under-damped second-order system (since that is the lowest order system which can oscillate). While the slower response would minimally be a first order system. That would lead one to conclude that at least a third order system is necessary to characterize this impulse response.

It is possible to estimate the order of the system required to model the impulse response shown in figure 6.1 by fitting progressively higher order systems to the impulse response and observing the order at which the estimate no longer improved. This was done using the method described by Ho and Kalman (1966), which fits a state model to a nonparametric impulse response. To determine how well an n^{th} order state model characterizes the nonparametric impulse response, an impulse response was computed from the state model and compared to the original nonparametric impulse response function. The result of such an analysis is shown in figure 6.2 which compares 2^{nd}, 3^{rd}, 4^{th}, and 5^{th} order impulse response functions.

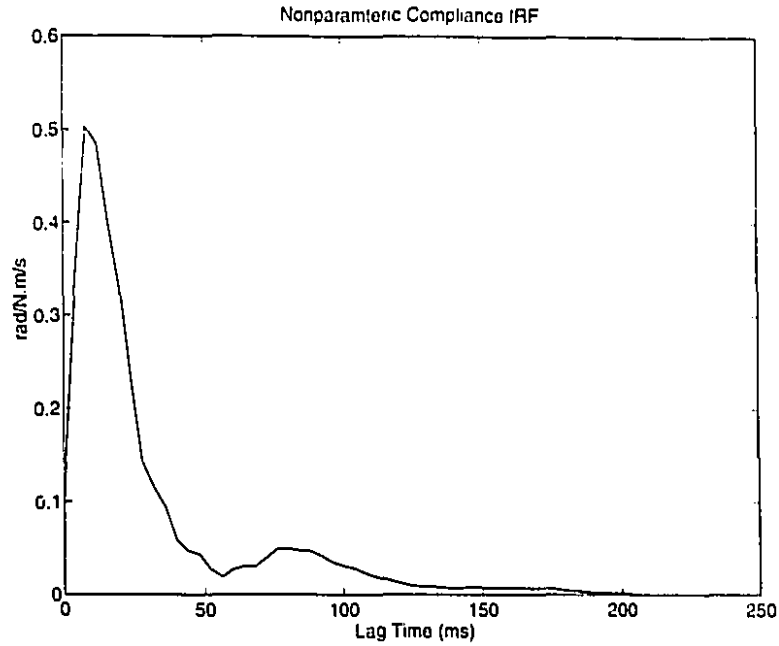

Figure 6.1. Nonparametric compliance impulse response, showing the state of the system at 250 ms after the onset of the twitch. This example is from data set three.

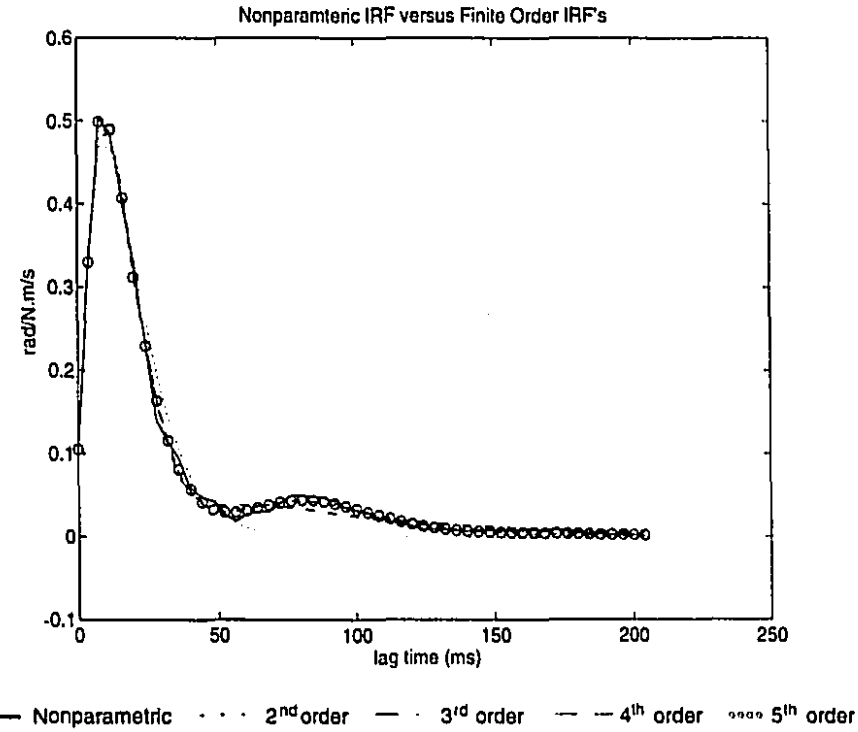

Figure 6.2. The same nonparametric impulse response as shown in figure 6.1, compared to finite order impulse response functions of progressively increasing order.

Figure 6.2 shows, qualitatively, that a finite order impulse response models the nonparametric impulse response better as the order of the impulse response increases. It is clear the second-order impulse response function does not capture the characteristics of the nonparametric impulse response functions. The third order impulse response function does better; it captures the under-damped second-order component, plus the slow first order component of the response.

The fourth order impulse response does better still, and, significantly, there is little observable difference between the fourth and fifth order impulse response functions. This lack of improvement from fourth to fifth order leads to the tentative conclusion that a parametric system model of at least order four is required to characterize this nonparametric impulse response function.

A quantitative estimate of system order is possible by choosing a measure of the difference between order n, and order n+1 impulse response functions. A logical choice for this function would be:

$$\Delta_n(t) = \frac{\sum\left(\hat{h}_{n+1}(t) - \hat{h}_n(t)\right)^2}{\sum\left(\hat{h}_n(t)\right)^2} \times 100 \qquad 6.1$$

where $\hat{h}_n(t)$ is the order n estimate of the nonparametric impulse response at time t through the time course of the twitch, and the sum is over each point in the impulse response.

This equation is simply 100 minus the variance accounted for between the finite order n impulse response, and the finite order $n+1$ impulse response. If the two impulse response functions were identical, the variance accounted for would be 100%, and equation 6.1 would be $\Delta_n = 0$. Therefore, one can expect that as n approaches the true system order, Δ_n will approach zero.

It is a simple matter to compute Δ_n for a range of system orders, n, at each point in time through the time course of the twitch. Figures 6.3, 6.4, 6.5, and 6.6 show the result of such an analysis. In each of these figures it is apparent that Δ_4 is the first point at which $\Delta_n(t) \approx 0$ for all values of time (i.e. through the entire time course of the twitch). This is persuasive evidence to support a hypothesis which suggests a fourth order model of joint dynamics.

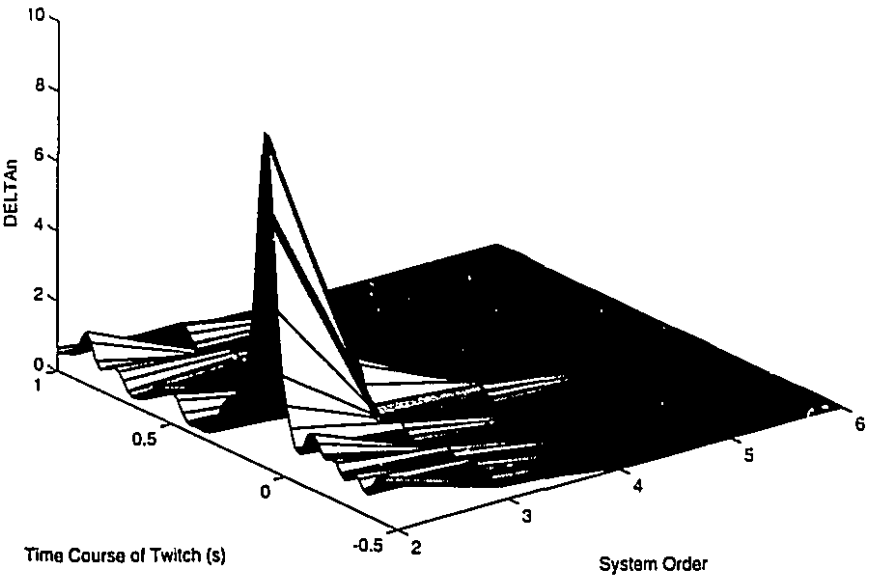

Figure 6.3. Δ_n versus n (system order) through the time course of the twitch for data set one.

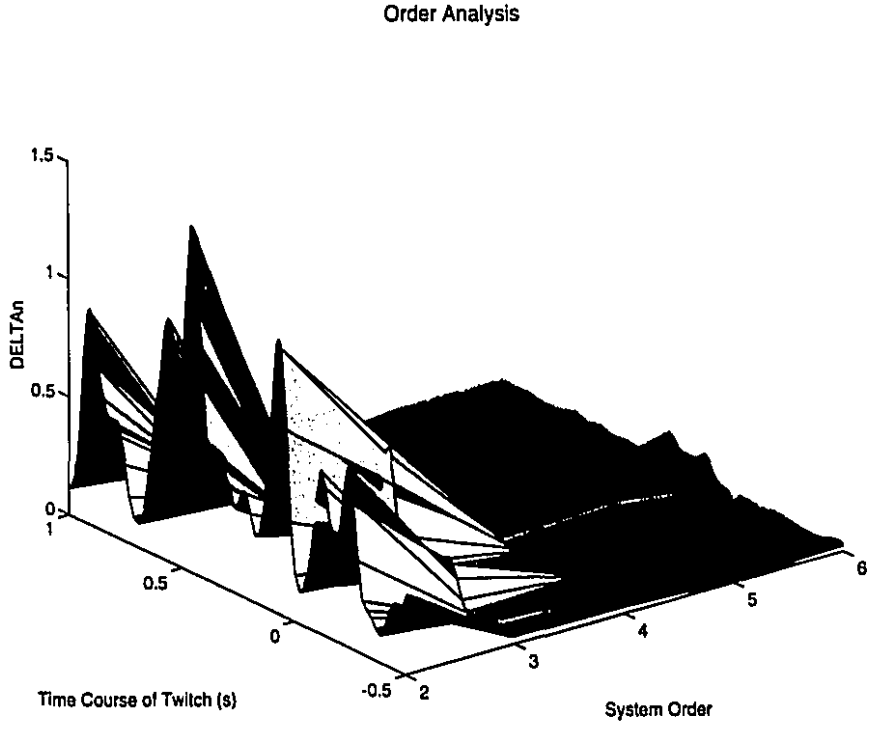

Figure 6.4. Δ_n versus n (system order) through the time course of the twitch for data set two.

Further, figures 6.3, 6.5, and 6.6 show that $\Delta_2 >> \Delta_4$ between approximately 0.0 (the onset of the twitch) and 0.5 seconds (the point of near full recovery). These characteristics suggest that the higher order dynamics only become significant during the time the muscle is actively contracting, and explain why the second-order model is successful under time-invariant conditions (i.e. before and after the twitch), but is less able to model joint dynamics under time-varying conditions. It does not seem unreasonable to suggest that this effect may also explain the second-order results presented by MacNeil et al. (1992), Kirsch et al. (1991, 1993), and Xu (1992).

7 Conclusions

Summary

The ensemble time-varying system identification approach was successful in identifying the dynamics of the ankle joint as they varied through a single twitch of the triceps surae muscle group. The ensemble method generates a nonparametric result that is not biased by any *a priori* assumptions, other than that of linearity, about the structure of the system under study. The stiffness impulse response functions presented in figures 5.8, 5.9, 5.10, and 5.11 form the basis from which study can continue with limited concern that basic assumptions about the nature of the system are wrong.

Nonparametric results are, however, very difficult to interpret in isolation. To gain further insight into the nature of the system, one approach is to characterize the results using parametric models. Parametric second-order models have been very successful in characterizing time-invariant joint dynamics (Kearney and Hunter, 1990). Second-order models have, however, met with less success in characterizing time-varying joint dynamics. This was found in the studies carried out by MacNeil et al. (1992), Kirsch et al (1991), and Xu (1992), and again in the work presented here.

Given the mounting evidence that a second-order linear model is not a useful means of characterizing time-varying joint dynamics, the question of what step to try next should be addressed. The first question addressed in the discussion was: is there an obvious reason why the second-order model fails during the time the system is varying (i.e., during the twitch). Simple visual examination of a single nonparametric compliance impulse response function representing the dynamics at a point in time when the system was varying leads one to conclude that the second-order model fails because a slower order dynamic becomes significant at this time. The impulse response remained oscillatory, but the oscillation is superimposed on the slower dynamic component. This implies that a system order higher than two is required to characterize joint dynamics when the system is time-varying.

A simple system order analysis was performed to determine the minimum system order required to characterize the nonparametric compliance impulse functions that represent the ankle joint dynamics at each point in time through the time course of the twitch. This analysis leads to the tentative conclusion that a system of at least order four is required to characterize the dynamics of the ankle joint under time-varying conditions.

Further, the analysis also predicts that a system order of two is sufficient during the time invariant periods before and after the twitch. This result is consistent with time-invariant studies which have concluded that a second order model is sufficient to characterize joint dynamics under time-invariant conditions, and at the same time explains why the second order model fails under time-varying conditions.

Future Directions

System order is an important consideration in the development of a model to characterize a system as complex as the neuromuscular system. Voluminous research has demonstrated that second-order models are sufficient to characterize joint dynamics under time-invariant conditions. The second-order model has, however, proved not wholly successful at characterizing the neuromuscular system under time-varying conditions. The conclusions presented here concerning system order are a basis for explaining the failure. It would be interesting to determine if an order analysis applied to the time-varying paradigms studied by MacNeil et al. (1992), and Kirsch et al, (1993) would give the same estimate of system order.

No theory capable of characterizing time-varying joint dynamics has been suggested in this thesis; developing such a theory is a formidable challenge, but the results do tentatively suggest some of the properties such a theory must possess:

- The model must be at least third, perhaps fourth, order
- Under time-invariant conditions, components of order greater than two should not be significant.
- Under time-varying conditions, components of order greater than two should become significant.

References

Bernotas, L. A., Crago, P. E., and Chizeck, H. J., A Discrete-Time Model of Electrically Stimulated Muscle, *IEEE Transaction on Biomedical Engineering*, **33**:829-837,1986

Bertonas, L. A., Crago, P. E., Chizeck, H. J., Adaptive Control of Electrically Stimulated Muscle, *IEEE Transaction on Biomedical Engineering*, **34**:140-147, 1987

Bendat, J. S., Piersol, A. G., Random Data Analysis and Measurement Procedures, John Wiley & Sons Inc., 1986

Bennet, D.J., Hollerbach, J. M., Hunter, I.W., Mechanical Properties of the Human Arm During Voluntary Movement, *Proceedings of the Canadian Medical and Biological Engineering Society Conference*, **16**:89-90, 1990

Bennet, D. J., Torques Generate at the Human Elbow in Response to Constant Position Errors Imposed During Voluntary Movement, *Exp Brain Res*, **95**:488-498, 1993

Carpenter, M.B., Human Neuroanatomy, seventh edition, 1976

Chia, T.L., Chow, P.C., Chizeck, H.J., Recursive Parameter Identification of Constrained Systems: An Application to Electrically Stimulated Muscle, *IEEE Transactions on Biomedical Engineering*, 38:429-442, 1991

Crago, P. E., Control of Movements By Functional Neuromuscular Stimulation, *Engineering in Medicine and Biology Magazine*, 32-36, Sept. 1983

Crago, P. E., Lemay, M., Active Regulation of Grasp Stiffness in a Neuroprosthesis for Restoration of Hand Function in Quadriplegics, *Transactions of the Annual International Conference of the IEEE Engineering in Medicine and Biology Society*, **11**:902-903, 1989

Crago, P.E., Lemay, M.E., Liu, L., External Control of Limb Movements Involving Environmental Interactions, In: Multiple Muscle Systems: Biomechanics and Movement Organization, Springer-Verlag, 343-359, 1990

Crago, P. E., Nakai, R. J., Chizeck, H. J., Feedback Regulation of Hand Grasp Opening and Contact Force During Stimulation of Paralyzed Muscle, *IEEE Transactions on Biomedical Engineering*, **38**:17-28, 1991

Gottlieb, G., L., Agarwal, G., C., Dependence of Human Ankle Compliance on Joint Angle, *J. Biomechanics*, **11**:177-181, 1978

Gerencsér, L., The Law of the Cubic Root, *Proceeding of the 9th IFAC/IFORS Symposium*, 63-65, 1991

Golub, G. H., Matrix Computations, The John Hopkins University Press, 1983

Hill, A. V., The Heat of Shortening and the Dynamics Constants of Muscle, *Proc. Roy. Soc. B.*, **126**:136-195

Ho, B. L., Kalman, R. E., Effective construction of linear, state-variable models from input/output functions, *Regellungstechnik*, **14**:545-548, 1966

Hogan, N., Adaptive Control of Mechanical Impedance by Coactivation of Antagonist Muscles, *IEEE Transaction on Automatic Control*, **AC-29**:681-690, 1984

Hogan, N., The Mechanics of Multi-Joint Posture and Movement Control, *Biological Cybernetics*, **52**:315-331., 1985

Hunter, I. W., Kearney, R. E., Dynamics of Human Ankle Stiffness: Variation With Mean Ankle Torque, *J. Biomechanics*, **15**:757-752, 1982

Hunter, I. W., Kearney, R.E., Two-sided Linear Filter Identification, *Medical & Biomedical Engineering and Computing*, **21**:203-209, 1983a

Hunter, I. W., Kearney, R. E., Invariance of Ankle Dynamic Stiffness During Fatiguing Muscle Contractions, *J. Biomechanics*, **16**:985-991, 1983b

Hunter, I. W., Korenberg, M. J., The Identification of Nonlinear Biological Systems: Wiener and Hammerstein Cascade Models, *Biol. Cybern.*, **55**:135-144, 1986

Hunter, I. W., Kearney, R. E., Quasi-Linear, Time-Varying, and Nonlinear Approaches to the Identification of Muscle and Joint Mechanics, In: Advanced Methods of Physiological System Modeling, Volume 1, Marmarelis, V. Z. (Ed.), pp. 128-147, 1987

Huxley, A. F., Muscular Contraction Review Lecture, *J. Physiol.*, **243**:1-43, 1974

Kalman, R.E., A New Approach to Linear Filtering and Prediction Problems, *Transactions of the ASME Journal of Basic Engineering*, **82D**:35-45., 1960

Kearney, R. E., Hunter, I. W., Dynamics of Human Ankle Stiffness: Variation With Displacement Amplitude, *J. Biomechanics*, **15**:753-756, 1982

Kearney, R. E., Hunter, I. W., Weiss, P. L., and Spring, K., Tilt-table/ankle-actuator system for the study of vestibulospinal reflexes. *Med. & Biol. Eng. & Comput.*, **21**:301-305, 1983

Kearney, R. E., Hunter, I. W., Nonlinear Identification of Stretch Reflex Dynamics, *Annals of Biomedical Engineering*, **16**:79-94, 1988

Kearney, R.E., Hunter, I.W., System Identification of Human Joint Dynamics, *Critical Reviews in Biomedical Engineering*, **18**:55-87, 1990.

Kearney R. E., Kirsch, R. F., MacNeil, J. B., Hunter, I. W., An Ensemble Time-Varying Identification Technique: Theory and Biomedical Applications, 9'th *IFAC/IFORS Symposium, Budapest, Hungary*, 191-196, 1991

Kirsch, R. F., Kearney, R. E., Time-Varying Identification of Human Ankle Joint Stiffness Dynamics During Imposed Movement, *Transactions of the Annual International Conference of the IEEE Engineering in Medicine and Biology Society*, **13**:2030-2031, 1991

Kirsch, R. F., Kearney, R. E., MacNeil, J B., Identification of Time-Varying Dynamics of the Human Triceps Surae Stretch Reflex (I. Rapid Isometric Contraction), *Exp Brain Res*, **97**:115-127, 1993

Lan, N., Crago, P. E., Chizeck, H. J., A Perturbation Control Strategy For FNS Motor Prostheses, *Transactions of the Annual International Conference of the IEEE Engineering in Medicine and Biology Society*, **12**:2327-2328, 1990

Lan, N., Crago, P. E., Chizeck, H. J., Control of End-Point Forces of a Multijoint Limb by Functional Neuromuscular Stimulation, *IEEE Transactions on Biomedical Engineering*, **38**:953-965, 1991a

Lan, N., Crago, P. E., Chizeck, H. J., Feedback Control Methods for Task Regulation by Electrical Stimulation of Muscles, *IEEE Transactions on Biomedical Engineering*, **38**:1213-1223, 1991b

Lawrence, P. J., Dawson, R. D., Identification of Periodic Nonstationary Antenna Stabilization Control Systems by Crosscorrelation Techniques, Proc. IEE, **124**:797-801, 1977

Ljung, L., System Identification for the User, Prentice Hall, 1987

Lacquaniti F., Licata, F., Soechting, J. F., The Mechanical Behavior of the Human Forearm in Response to Transient Perturbations, *Biol. Cybern.*, **46**:1226-1243, 1981

Lacquaniti, F., Carrozzo, M., Borghese, N. A., Time-varying Mechanical Behaviour of Multijointed Arm in Man, *Journal of Neurophysiology*, **69**:1443-1464, 1993

MacNeil, J. B., Kearney, R. E., Hunter, I. W., Time-Varying Identification of Human Joint Dynamics, *IEEE Engineering in Medicine & Biology Society 11th Annual International Conference*, 957-958, 1989

Marmarelis, P. Z., Marmarelis, V. Z., Analysis of Physiological Systems, Plenum Press, 1978

Marmarelis, V. Z., Practicable Identification of Nonstationary Nonlinear Systems, *IEE Proc. Part D*, **128**:211-214, 1981

Marmarelis, V. Z., Recent Advances in Nonlinear and Nonstationary Analysis, Advanced Methods of Physiological System Modeling, Volume 1, Marmarelis, V. Z. (Ed.), pp. 323-336, 1987

McMahon, T. A., Muscles, Reflexes, and Locomotion, Princeton University Press, 1984

MacNeil, J. B., Kearney, R. E., Hunter I. W., Identification of Time-Varying Biological Systems from Ensemble Data, *IEEE Transaction on Biomedical Engineering*, **39**:1213-1225, 1992.

Nichols, T. R., Houk, J. C., Improvement in Linearity and Regulation of Stiffness That Results From Actions of Stretch Reflex, *J. Neurophysiol.*, **28**:96-99, 1975

Press, W. H., Flannery, B. P., Teukolsky, S. A., and Vetterling, W. T., Numerical Recipes: The Art of Scientific Computing. UK: Cambridge Univ. Press, 1986

Schauf, C., Moffet, D., Moffet, S., Human Physiology, Foundations and Frontiers, Times Mirror/Mosby College Publishing, 1990

Soechting, J. F., Dufresne, J. R., Lacquaniti, F. (1981), Time-Varying Properties of Myotactic Response in Man During Some Simple Motor Tasks, *Journal of Neurophysiology*, **46**:1226-1243, 1981

Sorenson H. W., Least-squares estimation from Gauss to Kalman., *IEEE Spectrum*, **7**:63-68, 1970

Sorenson, H. W., Section I-B Theoretical Foundations, Kalman Filtering Theory and Application, Sorenson, H. W. (Ed.), IEEE Press, 1985

Strang, G., Linear Algebra and Its Application, second edition, 1980

Weiss, P. L., Kearney, R. E., Hunter, I. W., Position Dependence of Ankle Joint Dynamics — I Passive Mechanics, *J. Biomechanics*, **19**:727-735, 1986a

Weiss, P. L., Kearney, R. E., Hunter, I. W., Position Dependence of Ankle Joint Dynamics — II Active Mechanics, *J. Biomechanics*, **19**:737-751, 1986b

Weiss, P.L., Hunter, I.W., Kearney, R.E., Human Ankle Stiffness Over The Full Range of Muscle Activation Levels, *J. Biomechanics*, **21**:539-544, 1988

Westwick, D. T., Kearney, R. E., Identification of Multiple Input Wiener Systems, *Proceedings of the Annual International Conference of the IEEE Engineering in Medicine and Biology Society*, **12**:1895-1896, 1990

Wilkie, D. R., Facts and Theories About Muscle, *Proc. Biophysics*, **4**:288-324

Winters, J.M., Hill-Based Muscle Models: A Systems Engineering Perspective, In: Multiple Muscle Systems: Biomechanics and Movement Organization, Winters, J. M. (Ed.), pp. 69-93, 1990

Xu, Y., Hollerbach, J. M., Hunter, I. W., Time-Varying Identification of Elbow Joint Dynamics using Exponentially Weighted Least Squares, *Proceedings of the Annual International Conference of the IEEE Engineering in Medicine and Biology Society*, **13**:2020-2021, 1991a

Xu, Y., Hunter, I. W., Hollerbach, J. M., Bennet, D.J., An Airjet Actuator System for Identification of the Human Arm Joint Mechanical Properties, *IEEE Transaction on Biomedical Engineering*, **38**:1111-1122, 1991b

Xu, Y., Hollerbach, J. M., Hunter, I. W., An efficient Identification Method for Studying Time-Varying Joint Dynamics, *Proceedings of the Canadian Medical and Biological Engineering Society Conference*, **18**:34-35, 1992